

## CLAS12 Run Group A Jeopardy PAC52

### 11 GeV Polarized Electrons on Liquid Hydrogen Target to Study Proton Structure, 3D Imaging, and Gluonic Excitations

Harut Avakian, Nathan Baltzell, Sergey Boyarinov, Volker Burkert, Daniel S. Carman, Pierre Chatagnon, Raffaella De Vita, Chris Dilks, Latifa Elouadrhiri\*, François-Xavier Girod, Yuri Gotra, Valery Kubarovsky, Victor Mokeev, Rafayel Paremuzyan, Eugene Pasyuk, Patrizia Rossi, Youri Sharabian, Stepan Stepanyan, Maurizio Ungaro, Xiangdong Wei, Veronique Ziegler

*Thomas Jefferson National Accelerator Facility, Newport News, Virginia 23606, USA*

Marshall Scott, Maria Zurek

*Argonne National Laboratory 9700 S Cass Ave, Lemont, IL 60439, USA*

Carlos Ayerbe Gayoso, Keith Griffioen

*College of William and Mary, Williamsburg, Virginia 23187, USA*

David Heddle

*Christopher Newport University, Newport News, Virginia 23606*

Bill Briscoe, Isabella Illari, Axel Schmidt, Igor Strakovsky

*The George Washington University, Washington, District of Columbia 20052, USA*

Ralf Gothe, Yordanka Ilieva, Krishna Neupane, Steffen Strauch, Alexis Osmond

*University of South Carolina, Columbia, South Carolina 29208, USA*

Luca Barion, Marco Battaglieri, Mariangela Bondi, Andrea Celentano, Christopher Mullen, Mikhail Osipenko

*INFN, Sezione di Genova, 16146 Genova, Italy*

Andrea Bianconi

*Università degli Studi di Brescia, 25123 Brescia, Italy*

Giuseppe Ciullo, Marco Contalbrigo, Paolo Lenisa, Aram Movsisyan, Luciano Pappalardo

*INFN, Sezione di Ferrara, 44100 Ferrara, Italy*

Marco Mirazita, Orlando Soto, Matteo Turisini

*INFN, Laboratori Nazionali di Frascati, 00044 Frascati, Italy*

Marco Leali, Valerio Mascagna, Luca Venturelli

*INFN, Sezione di Pavia, 27100 Pavia, Italy*

Annalisa D'Angelo, Lucilla Lanza, Alessandro Rizzo

*INFN, Sezione di Roma Tor Vergata, 00133 Rome, Italy*

Alessandra Filippi

*INFN, Sezione di Torino, 10125 Torino, Italy*

Moskov Amaryan, Stephen Bueltmann, Mohammad Hattawy, Mariana Khachatryan, Jiwan Poudel  
*Old Dominion University, Norfolk, Virginia 23529, USA*

Carlos Salgado  
*Norfolk State University, Norfolk, Virginia 23504, USA*

Jixie Zhang  
*University of Virginia, Charlottesville, Virginia 22901, USA*

Phil Cole  
*Lamar University, 4400 MLK Blvd, PO Box 10009, Beaumont, Texas 77710, USA*

Lamiaa El Fassi, Shirsendu Nanda  
*Mississippi State University, Mississippi State, Mississippi 39762, USA*

Ahmed El Alaoui, Utsav Shrestha  
*Universidad Técnica Federico Santa María, Casilla 110-V Valparaíso, Chile*

Ryan Ferguson, Derek Glazier, Dave Ireland, Ian MacGregor, Bryan McKinnon, Daria Sokhan,  
*University of Glasgow, Glasgow G12 8QQ, United Kingdom*

Nicholas Zachariou  
*University of York, York YO10 5DD, United Kingdom*

Lei Guo, Brian Raue  
*Florida International University, Miami, Florida 33199, USA*

Maurik Holtrop  
*University of New Hampshire, Durham, New Hampshire 03824, USA*

Chaden Djalali, Ken Hicks, Gleb Fedotov  
*Ohio University, Athens, Ohio 45701, USA*

Richard Capobianco, Stefan Diehl, Timothy Hayward, Andrei Kim, Valerii Klimenko,  
Kyungseon Joo  
*University of Connecticut, Storrs, Connecticut 06269, USA*

Anselm Vossen, Zhiwen Zhao  
*Duke University, Durham, North Carolina 27708, USA*

Angela Biselli  
*Fairfield University, Fairfield, Connecticut 06824, USA*

Tony Forest  
*Idaho State University, Pocatello, Idaho 83209, USA*

Jerry Gilfoyle  
*University of Richmond, Richmond, Virginia 23173, USA*

Kevin Giovanetti, Gabriel Niculescu  
*James Madison University, Harrisonburg, Virginia 22807, USA*

Ivan Bedlinsky, Serguey Kuleshov, Oleg Pogorelko  
*Institute for Theoretical and Experimental Physics, Moscow 11759, Russia*

Natasha Dashyan, Hakob Voskanyan  
*Yerevan Physics Institute, 375036 Yerevan, Armenia*

Anna Golubenko, Evgeny Isupov  
*Skobeltsyn Nuclear Physics Institute, Moscow State University, 119899 Moscow, Russia*

Dominique Marchand, Silvia Niccolai, Eric Voutier  
*Institut de Physique Nucleaire, CNRS/IN2P3 and Universite Paris Sud, Orsay, France*

Hyon-Suk Jo  
*Kyungpook National University, Daegu 41566, Republic of Korea*

Francesco Bossù, Maxime Defurne, Franck Sabatie  
*Commissariat à l'Énergie Atomique Saclay, 91191 Gif sur Yvette, France*

Sangbaek Lee, Richard Milner  
*Massachusetts Institute of Technology, Cambridge, Massachusetts 02139, USA*

Fatiha Benmokhtar  
*Duquesne University, 600 Forbes Avenue, Pittsburgh, Pennsylvania 15282, USA*

Pawel Nadel-Turonski  
*Stony Brook University, 100 Nicolls Road, Stony Brook, New York 11794, USA*

James Ritman  
*Institute fur Kernphysik (Jülich), Jülich, Germany*

Nikos Sparveris  
*Temple University, Philadelphia, Pennsylvania 19122, USA*

**for the CLAS Collaboration**

\* Run Group Contact Person: Latifa Elouadrhiri - [latifa@jlab.org](mailto:latifa@jlab.org)



# Executive Summary

---

The CLAS12 Run Group A (RG-A) experiments were designed to carry out a series of complementary high-precision measurements aimed at elucidating the intricate structure of the proton across its ground and excited states, probing the proton's structure in three dimensions with unprecedented detail, and investigating gluonic excitations. The primary objective of this program is to unravel how the proton's fundamental constituents are held together by the strong force, to understand the emergence of the dominant part of hadron mass, and to perform precise extraction of the mechanical properties of the proton. The overarching ambition of the RG-A scientific agenda is to execute meticulous measurements that offer insights into the phenomenon of confinement. Over the last decade, major progress in the theoretical description of the interior structure of the nucleon has led to a breakthrough in our understanding of the theory of quarks and gluons in the regime of strong QCD. This, combined with the discovery of Generalized Parton Distributions (GPDs), has provided a novel way to describe nucleon structure in three dimensions (3D), two in the transverse coordinate space and one in the longitudinal momentum space. This discovery has opened up a new avenue of hadronic research that has become one of the flagship programs in nuclear and hadronic physics. The complementary process of semi-inclusive deep inelastic scattering (SIDIS) is also of topical interest in probing the internal structure of the nucleon in 3D momentum space. The science program of RG-A is very broad and encompasses in addition to 3D imaging, the study of the structure of the proton in its ground state, as well as in the many excited states both for baryons and for mesons, including the search for hybrids. These measurements will allow us to connect QCD to the early universe and to confinement. Extension of the CLAS  $N^*$  program in RG-A experiments toward the highest  $Q^2$  ever achieved in exclusive electroproduction will allow us to explore the emergence of the dominant part of the hadron mass and many facets of strong QCD underlying the generation of resonances of different structure.

The experiments require the reconstruction of exclusive or semi-inclusive processes, and hence the detection and reconstruction of mesons and baryons in the final state are vital. Other constraints come from the need for baryon and meson spectroscopy to measure complete angular distributions with precision. In many cases these processes are rare, therefore the measurements demand high luminosity and large acceptance detectors to map out the process in the full kinematic space using polarized beams, and with sufficiently high beam energy. CLAS12 with the 11-GeV beam, large acceptance, and operation at high luminosity  $\mathcal{L} = 10^{35} \text{ cm}^{-2}\text{s}^{-1}$  is ideal for this science program.

The RG-A science program is made up of 13 experiments driven by an international collaboration. These experiments have been grouped into six topical categories:

1. Deep Exclusive Processes (E12-06-119, E12-06-108, and E12-12-007): *Study of Generalized Parton Distributions (GPDs), 3D imaging of the proton, and study of its gravitational and mechanical structure*
2. Deep Inclusive and SIDIS (E12-06-112, E12-06-112A, and E12-06-112B): *Study of the Transverse Momentum Distributions (TMDs) and the 3D structure in momentum space*
3. Quasi-Photoproduction (E12-12-001 and E12-12-001A): *Study of  $J/\psi$  photoproduction, LHCb pentaquarks, and timelike Compton scattering*
4. Nucleon Structure (E12-09-003, E12-06-108A, and E12-06-108B): *Study of nucleon resonance structure at photon virtualities  $Q^2$  from 2.0  $\text{GeV}^2$  to 12  $\text{GeV}^2$*
5. MesonEx Program (E12-11-005) *Study of meson spectroscopy in the search for hybrids*
6. VeryStrange Program (E12-11-005A): *Photoproduction of the very strangest baryons on a proton*

The total RG-A PAC-approved days amount to 139. With 32 days taken in spring 2018, including 3-pass running and special detector/trigger setups dedicated to CLAS12 spectrometer commissioning runs, along with 29 days in fall 2018, and 19 days in spring 2019, we have expended a total of 74 PAC days. Consequently, there are 65 days of approved PAC beam time remaining to ensure the successful completion of the RG-A scientific program.

The charge collected so far, shared with the other RG-A experiments, corresponds to approximately 53% of the total originally approved beam time. While our data analyses are underway and initial papers have been published, it is crucial to emphasize that unlocking the full potential of the RG-A science program critically depends on maximizing our remaining beam time. This document provides a comprehensive update on scientific progress and data analysis across key experiments of the RG-A science program, highlighting the urgent need to maintain our remaining beam time to fully achieve our research objectives.

# 1 Deep Exclusive Processes (E12–06–119, E12–06–108, and E12–12–007)

## 1.1 Introduction

Generalized Parton Distributions (GPDs) [BR05; Die03; KLM16] unify the concepts of Form Factors (FFs) and Parton Distribution Functions (PDFs), and encode information on new hadronic matrix elements of local QCD operators such as the Energy Momentum Tensor (EMT) of quarks and gluons inside the nucleon [PS18]. Exploring GPDs in the valence region is one of the main goals of the JLab 12 GeV upgrade and one of the central deliverables for CLAS12 [Bur18].

We express the experimental observables of DVCS in terms of Compton Form Factors (CFFs) [BM10]. Using fixed  $t$  dispersion relations, we get the real parts of the CFFs as a function of their imaginary parts and the  $D$ -term.  $D(0)$  can be considered the last global unknown of the nucleon, a fundamental “gravitational charge” derived from the conserved currents of this bound state, at the same level as its mass, spin, electric charge, magnetic moment, or axial coupling constant [PS18]. New questions arise, such as how the mechanical radius of these force distributions compares to its electrical or mass radii.

The completion of the GPD program necessitates the analysis of DVMP where the produced meson filters quantum numbers and disentangles different flavors. Pseudoscalar meson production is sensitive to chiral odd or transversity GPDs, coupling to twist-3 chiral odd meson transversity Distribution Amplitudes through a quark helicity flip [AGL09].  $DV\pi^0$  and  $\eta$  production, being dominated by the transverse amplitude, determine these transversity GPDs. They probe novel spin orbit structures, such as the deformation of the quark impact parameter distributions depending on the quark or nucleon spin. Comparisons between chiral even and chiral odd GPDs provide tests for models of dynamical chiral symmetry breaking in QCD.

Although the exclusive program at JLab at 12 GeV is primarily geared towards the valence region, a substantial amount of gluons can still contribute to certain exclusive processes, allowing us to probe the nucleon gluonic structure similarly to the quark measurements. One such process is Deep Exclusive  $\phi$  production. No new data on  $DV\phi P$  have been published since the approval of E12–12–007.

## 1.2 Deeply Virtual Compton Scattering (E12–06–119)

The Deeply Virtual Compton Scattering  $ep \rightarrow e'p\gamma$  beam spin asymmetries (BSAs) were published in PRL **130**, 211902 (2023). They include data at 10.2 and 10.6 GeV. Novel methods were developed both for the separation of the signal and the background, as well as for the extraction of the BSA observables. Comparisons with models and global fits [KLM16] for a few bins are shown in Fig. 1. Mild tension between the published data and global fits KM15 [KLM16] (shown as the green dashed-dotted curves in the plots) can be seen as  $Q^2$  increases. This discrepancy is most noticeable around  $\phi = 90^\circ$  and  $270^\circ$ , where the asymmetry reaches its maximum values, and is significant at a few standard deviations. Given the state of the comparison between the current data and the best global fit available [KLM16], even a moderate improvement in uncertainties, or a slight change in measured values, could have a significant impact on the interpretation of these results, it therefore seems crucial for the remaining approved beam time to be collected in a timely manner.

## 1.3 Hard Exclusive Electroproduction of $\pi^0, \eta$ (E12–06–108)

The first measurements of beam spin asymmetries for the deeply virtual  $\pi^0$  electroproduction channel from the RG-A experiment with CLAS12 were published in Phys. Lett. B, and their comparisons with GPD-based theoretical models indicate dominant contributions from the chiral-odd GPDs even at the extended kinematic range facilitated by the 12 GeV upgrade (see Fig. 2). The additional beam time will allow for reduction of the statistical uncertainties of the measurements, providing strong constraints on the chiral-odd

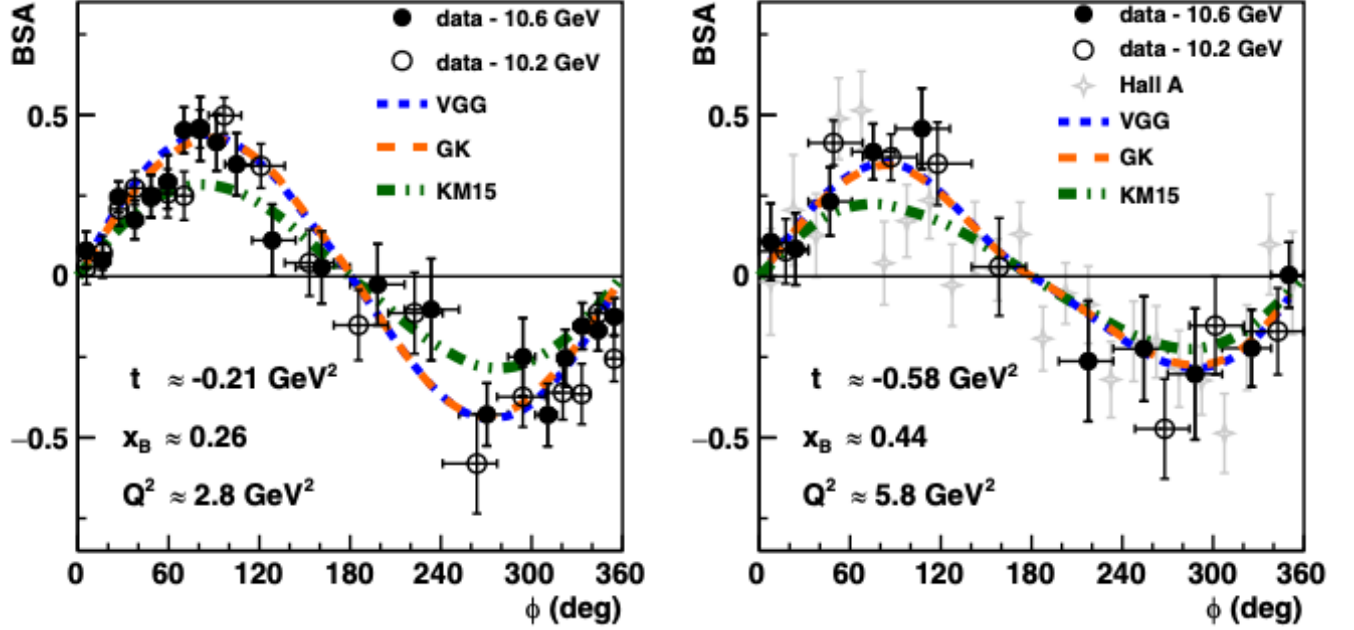


Figure 1: DVCS published BSA at 10.2 and 10.6 GeV. Mild tensions with the KM15 global fit, with discrepancies comparable with the current uncertainties, can be observed.

GPD  $\bar{E}_T$ , which is sensitive to the nucleon’s anomalous magnetic moment. The extractions of unpolarized cross sections are at the advanced analysis stage, and will also benefit from an expanded dataset.

#### 1.4 Exclusive $\phi$ Meson Production (E12–12–007)

Deep exclusive  $\phi$  meson electroproduction in the valence region is of special significance in the overall exclusive program as a probe of the gluonic GPDs. The “gluonic form factor” reveals the transverse spatial distribution of gluons in the nucleon’s valence region. The primary goal of this proposal is to measure the *relative* dependence of  $\frac{d\sigma_L}{dt}$ : only the  $t$  dependence is required, with overall normalization factor at  $t = 0$  (or  $t = t_{min}$ ). We will first quantify the approach to the regime of small-size configurations at high  $Q^2$  by testing model-independent features of the reaction mechanism, such as the  $Q^2$  scaling of cross sections and  $t$  slopes, the change of  $W$  dependence with  $Q^2$ , the  $L/T$  ratio obtained from  $\phi \rightarrow KK$  angular decay analysis and response functions. Then we will extract the gluonic size in the valence region from the relative  $t$ -dependence of  $\frac{d\sigma_L}{dt}$ , both model-independently ( $x$ -averaged size) and with information from GPD-model based calculations ( $x$ -dependent size).

We illustrate preliminary results from the spring 2019 data analysis (see Fig. 3). We selected events in the channel  $ep \rightarrow e'pK^+K^-$  with all particles detected. Standard procedures for particle identification and data quality, as detailed in the RG-A analysis note, are applied. We also apply standard DIS cuts,  $Q^2 > 1.5 \text{ GeV}^2$ ,  $W > 2 \text{ GeV}$ . In addition we apply a series of exclusive selection cuts: for each hadron we apply wide cuts around the missing mass and the missing direction of the hadron compared to the detected hadron momentum. We also apply wide cuts on the energy, mass, and momentum transverse to the beam to the total missing system  $ep \rightarrow e'pK^+K^-X$ . We illustrate the results of the exclusive selection cuts on the left in Fig. 3. For brevity, we only show the proton missing mass. Similarly clean exclusive peaks are identified in all these spectra. To cleanly separate our sample from the remaining spectra, we use the invariant mass of the kaon pair, illustrated on the right in Fig. 3. A clear prominent peak is shown at the expected position, above a significant background. We perform a fit to this invariant mass lineshape to estimate our exclusive counts. The best figure of merit for our lineshape is given for a region of about  $2\sigma$

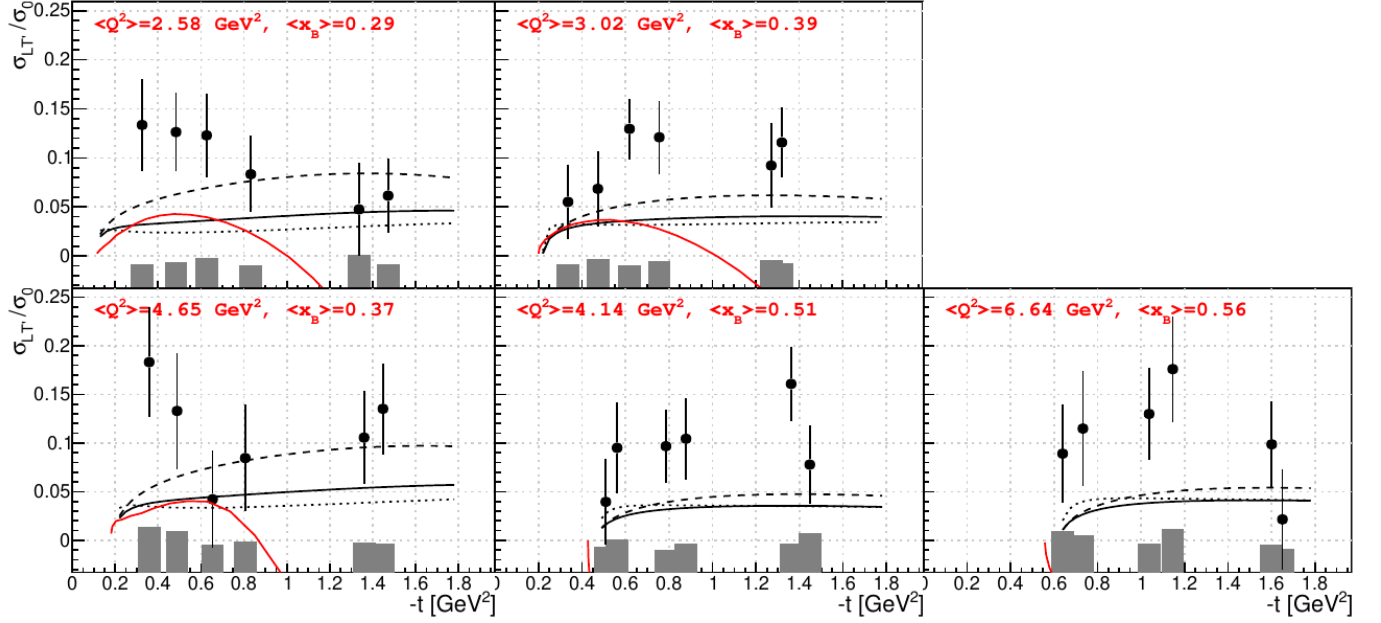


Figure 2: The measurements of  $\sigma_{LT}/\sigma_0$  and its statistical uncertainty for  $\pi^0$  as a function of  $-t$  in the forward kinematic regime. The gray bins represent the systematic uncertainties. The black curves show the theoretical prediction from the GPD-based Goloskokov-Kroll model. The black dashed lines show the effect of the GPD  $\bar{E}_T$  multiplied by a factor of 0.5, and the black dotted lines show the effect of the GPD  $H_T$  multiplied by a factor 0.5. The red curve shows the theoretical predictions from the Regge-based JML model.

around the signal peak.

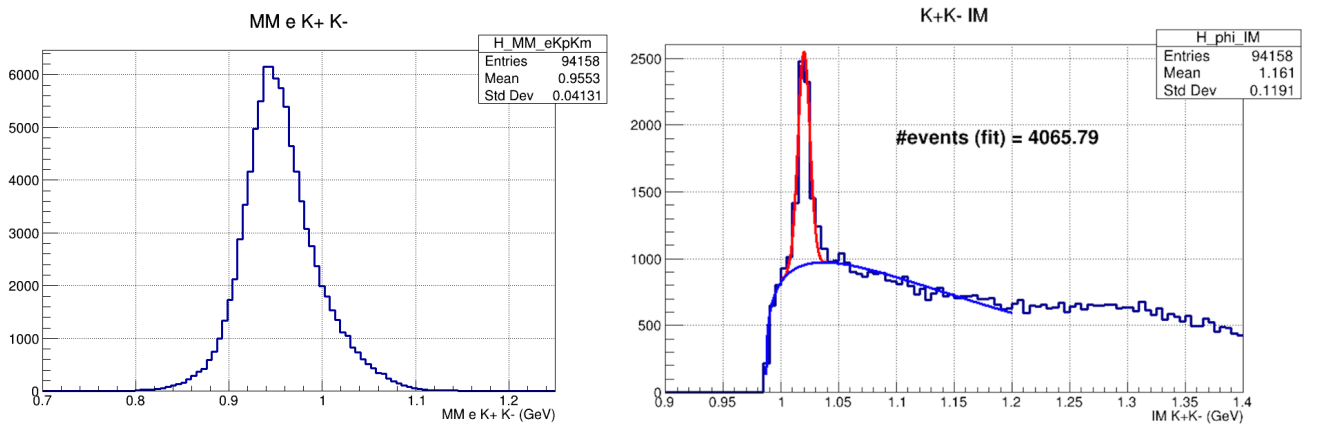


Figure 3: Selection of the exclusive  $\phi$  meson production in the spring 2019 data. Left: proton missing mass  $ep \rightarrow e'K^+K^-X$ . Right:  $K^+K^-$  invariant mass after selection cuts for the exclusive  $\phi$  meson production.

Exclusive  $\phi$  meson production offers a unique opportunity to probe the gluon spatial distribution and to compare the gluon radius to the quark radius in the valence region. This also places our exclusive program to complement the future collider program, which will focus on the sea region with high precision. The statistics for the identification of this channel with all particles detected is more challenging than for exclusive processes on quarks in the valence region, as expected. In order to properly estimate the ratio

$R = L/T$  of the relative contributions to the unpolarized cross section, we need to perform an angular decay analysis of the  $\phi$ . We also need to check for the dependence of this ratio against various kinematics. It is therefore crucial for the full realization of this part of the program that all the data originally approved be collected.

## 1.5 Hard Exclusive $\rho$ Meson Electroproduction

The measurements of beam spin asymmetries for the deeply virtual  $\rho$  electroproduction channel have been submitted for internal Collaboration review and show a particularly interesting feature of a sign change when observing the higher  $-t$  range (see Fig. 4). For vector meson channels, the measurements of decay products allow the extraction of Spin Density Matrix Elements (SDMEs), providing more experimental model-independent constraints for GPD-based calculations. Their analysis, however, introduces additional kinematic variables, which increases the reliance of exclusive vector meson analysis on statistics even further.

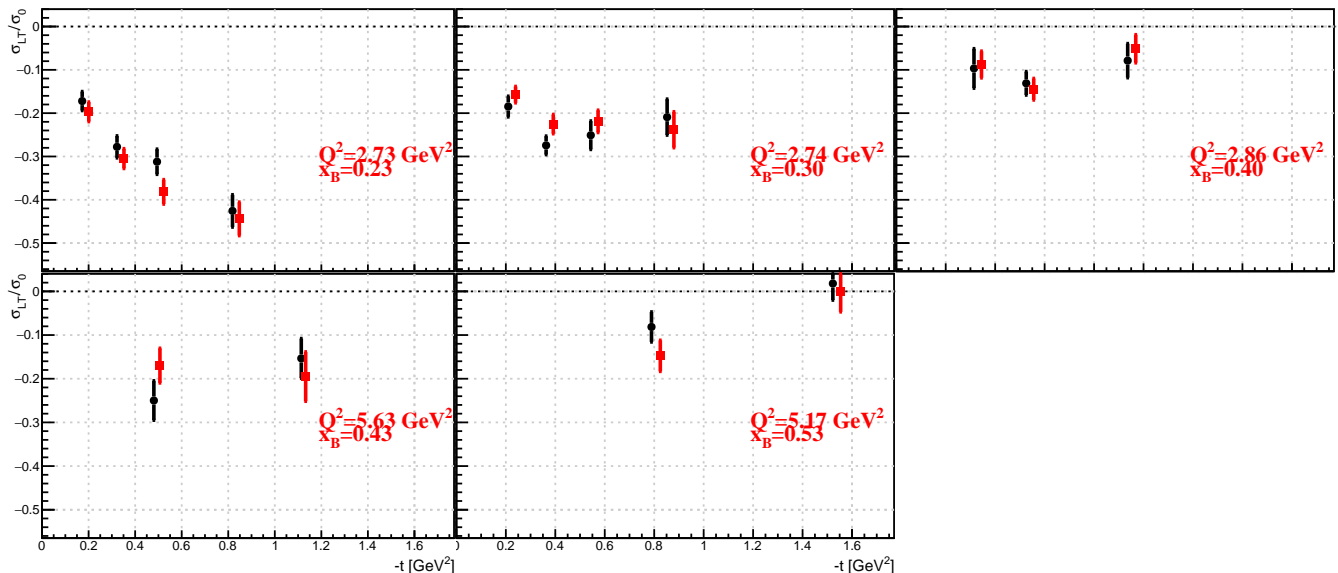


Figure 4: The measurements of  $\sigma_{LT'}/\sigma_0$  for  $\rho$  meson electroproduction for multi-dimensional binning: 5  $\{Q^2, x_B\}$  bins and multiple  $-t$  bins within each  $\{Q^2, x_B\}$  bin.

## 1.6 Deeply Virtual Pion Production and $N \rightarrow N^*$ DVMP

For the hard exclusive DVMP electroproduction channels  $ep \rightarrow e'X$ , with  $X = \pi^+n$ ,  $\pi^0p$ , and  $\pi^-\Delta^{++}$ , the polarized cross section ratio  $\sigma_{LT'}/\sigma_0$  has been extracted based on beam-spin asymmetry measurements using a 10.2 GeV and 10.6 GeV incident electron beam with RG-A (see Fig. 5). While  $\pi^+n$  and  $\pi^0p$  can be related to transversity GPDs,  $\pi^-\Delta^{++}$  provides the first observable sensitive to  $p \rightarrow \Delta$  transition GPDs.

For  $\pi^+n$  a fully differential study ( $Q^2$ ,  $x_B$ ,  $-t$ ,  $\phi$ ) in the GPD regime (low  $-t$ ) was possible based on  $e'\pi^+X$  using the missing mass technique, and allowed for detailed comparisons to GPD-based models. However, a study of the transition distribution amplitudes (TDAs) under backward kinematics ( $u$  channel) will require the detection of all final state particles for a clean background rejection and therefore more statistics will greatly help to perform a fully differential study in this kinematic regime.

For  $\pi^0p$  all final state particles need to be detected to obtain a clean event reconstruction. Therefore, the statistical uncertainties and bin sizes in the relevant kinematic variables of a fully differential study are

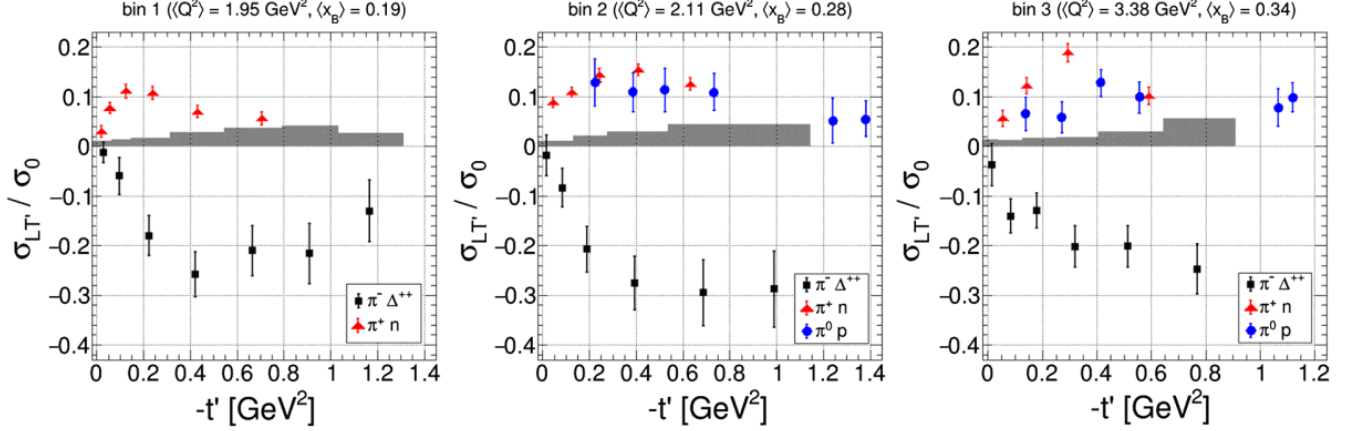


Figure 5:  $\sigma_{LT'}/\sigma_0$  and its statistical uncertainty for  $\pi^- \Delta^{++}$  (black squares) as a function of  $-t'$  in the forward kinematic regime and its systematic uncertainty (gray band). The subfigures correspond to the results for different  $Q^2$  and  $x_B$  bins. In addition, the results from the hard exclusive  $\pi^+ n$  (red triangles) and  $\pi^0 p$  (blue circles) electroproduction with similar kinematics are shown. Figure from Phys. Rev. Lett. 131, 021901 (2023).

still quite large with the presently available statistics. For this channel, more statistics will allow much more precise studies with a finer binning and a better comparison to theoretical models.

The study of  $\pi^- \Delta^{++}$  shows similar statistical limitations. Here, only three  $Q^2$ - $x_B$  bins could be separated to keep the statistical uncertainties at a reasonable level. Also here more statistics will help to perform a finer multi-dimensional binning and to reduce the statistical uncertainties. In addition, a binning in terms of the decay kinematics of the resonance, in addition to the other variables, will greatly improve the capabilities for an extraction and separation of the transition GPDs. Here, at least an order of magnitude more statistics would be greatly beneficial. For all listed DVMP channels, the same arguments hold also for cross section extractions, which are currently ongoing.

## 1.7 Accessing Pion GPDs Through Sullivan DVCS

The 3D structure [Bur00] of the pion can be accessed through GPDs. Throughout the years, many models for pion GPDs have been developed. They rely on various physics assumptions and, if feasible, Deep Virtual Compton Scattering (DVCS) [Ji97a] off the pion would provide key constraints on these models [Ber+21; Ber+22; Cha+22]. Using the data collected with CLAS12, we propose to study the pion structure through the Sullivan process introduced in Ref. [ADL08] and characterized by  $ep \rightarrow e'n\pi^+\gamma$ .

The analysis was performed with data collected in fall 2018 and spring 2019. Events with an electron, a positive pion, and a high-energy photon were selected. The missing mass associated with  $ep \rightarrow e'\gamma\pi^+X$  was calculated and a cut was applied to ensure exclusivity.

For a proper interpretation of the event as a Sullivan DVCS process, the pion virtuality  $|t|$  was required to be small enough such that  $|t| \leq |t|_{max} = 0.7 \text{ GeV}^2$ ,  $|t_\pi| \leq 0.7 \text{ GeV}^2$ ,  $Q^2 > 1 \text{ GeV}^2$ , and  $s_\pi = (p_\pi + q)^2 > s_\pi^{min} = 1.08 \text{ GeV}^2$ . In addition, to reduce the contribution from nucleon resonances  $N^*$  through the process  $ep \rightarrow e'N^*\gamma \rightarrow e'n\pi\gamma$ , the invariant mass of the  $n\pi$  system was required to be larger than 1.5 GeV.

With this selection, a non-zero beam-spin asymmetry is observed as seen in Fig. 6 when integrated over the entire phase space. However, the statistics is limited and would greatly benefit from the remaining beam time requested initially for RG-A. This additional statistics would allow us to perform refined studies regarding possible resonance contributions or to refine the binning.

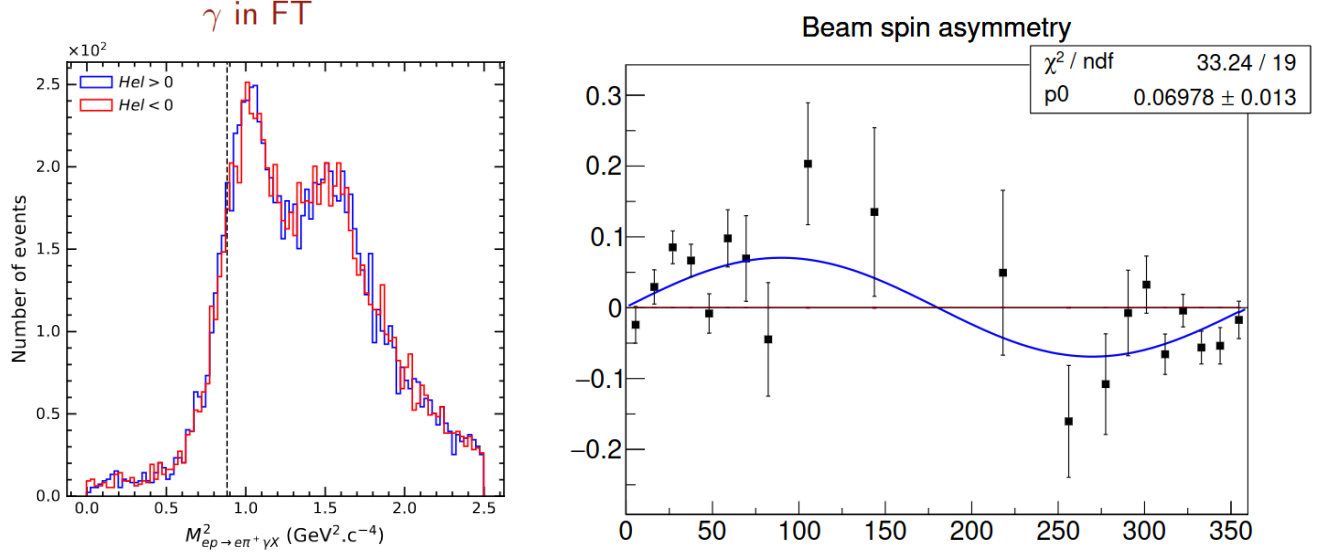


Figure 6: Left: Missing mass  $ep \rightarrow e'\gamma\pi^+X$  for both helicity states with the photon in the Forward Tagger. To select the Sullivan DVCS events, a cut at 1.2 GeV<sup>2</sup> is applied. Right: Beam-spin asymmetry for  $ep \rightarrow e'\gamma\pi^+n$  with the kinematical cuts introduced above.

## 1.8 The $N \rightarrow N^*$ DVCS Process

Another channel, which can be used to study  $N \rightarrow N^*$  transition GPDs, is the  $N \rightarrow N^*$  DVCS reaction,  $ep \rightarrow e'N^*\gamma \rightarrow e'n\pi^+\gamma$ . With this process, direct access to the so far experimentally not constrained twist-2 transition GPDs becomes possible. Transition GPDs will enable us to do a 3D imaging of baryon resonances and of the excitation process and to relate the angular momentum of resonances, as well as the pressure distribution within resonances, to the motion and distribution of the partons.

For the measurement of the  $N \rightarrow N^*$  DVCS process, all final state particles need to be detected. Based on the statistics already collected with RG-A, a differential study is only possible in one kinematic variable, in addition to the  $\phi$  dependence, with relatively large uncertainties. Within these uncertainties, ongoing studies of the process showed a good agreement with theoretical predictions. Any increase in statistics would greatly help to improve the measurement of this channel. A fully differential study in terms of the seven independent kinematic variables, including the resonance decay properties, would require an increase in statistics of at least 1 to 2 orders of magnitude. However, an increase of a factor 2 to 3 would already help to significantly improve the results of first studies and theory comparisons, which will motivate more precise studies in the future.

## 2 Semi-Inclusive Production of Pions (E12-06-112 and E12-06-112A)

Semi-inclusive deep inelastic scattering (SIDIS) is a powerful tool that enables us to study the momentum space tomography of nucleons and nuclei through a range of quantum correlation functions in QCD such as transverse-momentum dependent PDFs (TMDs). Although the study of SIDIS cross sections provides invaluable insight into hadron structure, the complexity of these cross sections poses significant experimental and phenomenological challenges. With up to 18 structure functions (SFs) to consider [Bac+07] (depending on the relevant degrees of freedom, such as beam and target polarizations), each structure function offers unique information about quark-gluon dynamics in the nucleon. These structure functions have intricate kinematic dependencies, such as  $x$ ,  $Q^2$ , and  $P_T$ , and measuring each one requires the full  $\phi$  dependence of the reaction and, in some cases, the  $\epsilon$  dependence, which defines the relative cross section contributions from

longitudinal ( $\sigma_L$ ) and transverse photons ( $\sigma_T$ ).

Most of the current SIDIS programs have mainly focused on studying SFs related to transversely polarized virtual photons. Unfortunately, longitudinal SFs have not received much attention and their contribution to the phenomenology of TMDs remains largely unexplored. This lack of understanding of longitudinal photon contributions introduces systematic uncertainties that can only be evaluated through direct measurements, combining the RG-K and RG-A datasets.

Assuming single-photon exchange, the SIDIS cross section for polarized beam and unpolarized targets, which are the main focus of RG-A, can be decomposed into a sum of various azimuthal modulations coupled to corresponding structure functions. The SIDIS cross section has the following form [Kot95; MT96; Bac+07]:

$$\frac{d\sigma}{dx dy d\zeta dP_T^2 d\phi_h} = \hat{\sigma}_U \left\{ F_{UU} + \sqrt{2\varepsilon(1+\varepsilon)} F_{UU}^{\cos\phi_h} \cos\phi_h + \varepsilon F_{UU}^{\cos 2\phi_h} \cos 2\phi_h + \lambda_\ell \sqrt{2\varepsilon(1-\varepsilon)} F_{LU}^{\sin\phi_h} \sin\phi_h \right\}. \quad (1)$$

Multiplicities, defined by the structure function  $F_{UU,T}$ , are a fundamental measurement of particle physics, detailing the fraction of production of a particle species within a more general production process. The motivation of this work is to use SIDIS to measure neutral pion production in a five-dimensional kinematic phase space, *i.e.*,  $x, Q^2, z, P_T^2$ , and  $\phi_h$ . Hadronization cannot be described solely with perturbative methods and so the interaction is factorized into the convolution of the electromagnetic hard scattering cross section and a series of non-perturbative PDFs and Fragmentation Functions (FFs). Measuring these multiplicities provides insight into the nature of hadronization through these FFs. Moreover, the  $P_T^2$  dependence of the multiplicities provides information on quark transverse momenta within the proton. Lastly, because neutral pions possess the average quark-antiquark content of the two charged pions, neutral pion multiplicities also provide information for charged pion multiplicities, and consequently, charged pion FFs.

Currently, the  $\phi_h$  integrated neutral pion multiplicities have been extracted from 64  $z - P_T^2$  bins within each of 8  $x - Q^2$  bins. The  $P_T^2$  integrated multiplicities have also been extracted within each of the 8  $x - Q^2$  bins and compared to the calculations of the Leading Order (LO) theory using the CT10nlo PDF sets convoluted with the MAPFF and the NNFF FFs. The individual  $P_T^2$  and fully integrated  $P_T^2$  multiplicities, as a function of  $z$ , for the first  $x - Q^2$  bin are shown in Fig. 7. The integrated multiplicities are consistent with predictions from the LO theory.

First preliminary measurements of the  $\cos\phi$  ( $F_{UU}^{\cos\phi}$ ) and  $\cos 2\phi$  ( $F_{UU}^{\cos 2\phi}$ ) moments of the unpolarized SIDIS inclusive  $\pi^+$  cross section have been extracted from the acceptance corrected  $\phi_h$  distributions as a function of  $z$  and plotted in separate  $P_T$  bins for a particular region of  $Q^2$  and  $y$  (see the highlighted bin in  $Q^2$  vs.  $y$  in Fig. 8). This example shows the measurements taken from the pass-1 version of the RG-A fall 2018 inbending data using the  $ep \rightarrow e'\pi^+ + X$  SIDIS reaction. The data is currently corrected only for acceptance and bin migration using a multi-dimensional Bayesian unfolding method, simultaneously unfolded in  $z$ ,  $P_T^2$ , and  $\phi_h$ . No other corrections (including radiative corrections) have been included yet. The observed trends are that the magnitude of the  $\cos\phi$  moments seems to increase with  $P_T$ , yet stays relatively consistent across varying  $z$ , while the  $\cos 2\phi$  moments appear to favor more positive values at higher  $P_T$ , while also seeming to converge toward zero at higher values of  $z$ . These trends appear to be consistent with those observed in other regions of  $Q^2$  and  $y$ , although these findings remain preliminary due to the incomplete application of necessary corrections and due to the use of the pass-1 version of the data files instead of the more recent pass-2 versions (currently in the process of switching this analysis to pass-2).

Measurements of hadron pairs in multi-dimensional space is critical for understanding the systematics of inclusive hadron SIDIS, and at the same time providing access to studies of hadronic and partonic correla-

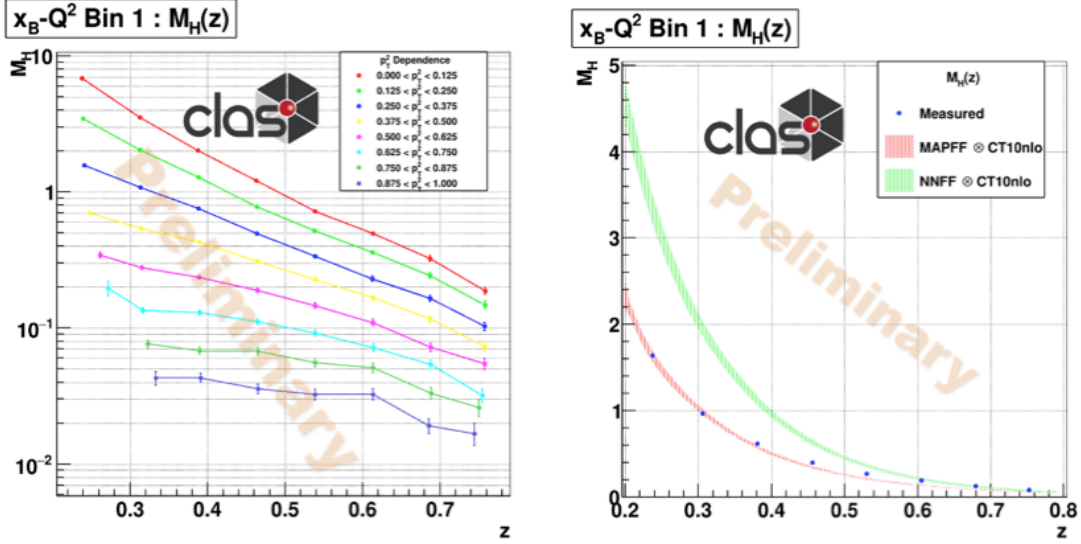


Figure 7: Neutral pion multiplicities as a function of  $z$  for the 8  $P_T^2$  bins (left) and  $P_T^2$  integrated multiplicities with the associated LO theory curves (right). In the right plot, the measured data is depicted in blue and the LO theory curves using the MAPFF and NNFF FF are depicted in red and green, respectively. Only statistical uncertainties are shown and the error bands on the theory curves represent a 68% confidence interval.

tions, not accessible with single hadrons. Beam spin asymmetries for SIDIS dihadrons provide information on multiple distributions, namely, dihadron fragmentation functions (DiFFs) and collinear twist-3 PDFs  $e(x)$ . The initial measurement of  $\pi^+\pi^-$  dihadron beam spin asymmetries [Hay+21] allowed for the first point-by-point extraction of the valence-quark  $e(x)$  distribution [Cou+22], as well as a first look at the behavior of the longitudinal spin-dependent DiFF  $G_1^\perp$ , which appears to exhibit a sign change around the  $\rho$ -meson mass. Extending this analysis with a partial wave expansion will give access to the correlation between the fragmenting quark angular momentum with the angular momentum of the dihadron, offering further constraints on the DiFFs. Furthermore, different dihadron channels probe different DiFFs, while a comparison of the asymmetries from a proton target (RG-A) to those of a deuteron target (RG-B) gives access to the flavor dependence of  $e(x)$ . These analyses are well underway for multiple dihadron channels; preliminary results for  $\pi^+\pi^-$  dihadron partial waves are shown in Fig. 9. In contrast to single-hadron measurements, dihadrons require an extra particle along with additional degrees of freedom, thus more data are needed to achieve similar precision as the single-hadron results; more RG-A data would allow for finer multi-dimensional binning, and thus improved constraints on the underlying PDFs and DiFFs.

### 3 Timelike Compton Scattering and $J/\psi$ Photoproduction (E12-12-001 and E12-12-001A)

The aim of both the E12-12-001 and E12-12-001A experiments is to study exclusive lepton pair photoproduction on the proton target  $\gamma p \rightarrow l^-l^+p$ , where  $l^-/l^+$  can be  $e^-/e^+$  or  $\mu^-/\mu^+$ . The exclusiveness of the reaction is achieved through the missing four-momentum analysis of  $e^-p \rightarrow l^-l^+p+X$  or  $e^-p \rightarrow l^-l^+e^-+X$  by requiring the missing mass to be close to 0 or close to the proton mass for the latter case. Here, for the  $l^-l^+e^-$  topology,  $e^-$  is the beam scattered electron detected in the Forward Tagger (FT) of CLAS12 [Bur+20]. Timelike Compton Scattering (TCS) and  $J/\psi$  photoproduction near the energy threshold are the primary physics processes investigated through exclusive photoproduction of lepton pairs. RG-A collected

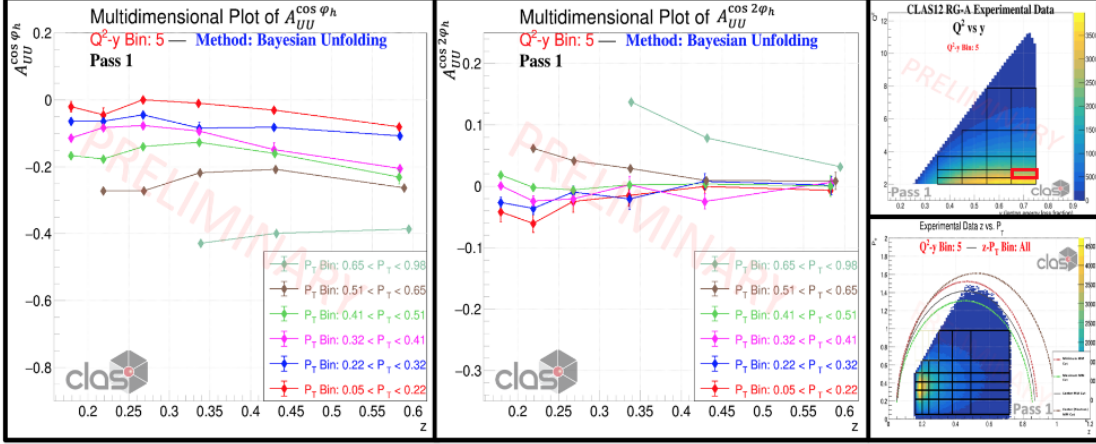


Figure 8: Measurements of  $\cos \phi$  and  $\cos 2\phi$  modulation in inclusive  $\pi^+$  production in SIDIS.

data in the spring and fall of 2018 with 10.6 GeV electron beams and in the spring of 2019 with a beam energy of 10.2 GeV. Additionally, in the fall of 2018, RG-A took data with both polarities of the CLAS12 torus magnet.

Since the previous jeopardy update in the summer of 2020, significant developments in data analysis and improvements in data reconstruction quality (efficiency, resolution, etc.) have occurred. In particular, Pierre Chatagnon successfully defended his Ph.D. thesis on TCS in October 2020, and Joseph Newton's Ph.D. thesis on  $J/\psi$  photoproduction near the energy threshold was defended in August 2021. The paper based on Pierre's Ph.D. thesis has been published in Physical Review Letters (PRL), and the analysis of the  $J/\psi$  production cross section near threshold is being finalized. We expect to release the results in 2024. Currently, two Hall-B postdocs, Pierre Chatagnon and Richard Tyson, along with Ph.D. student Mariana Tenorio Pita from Old Dominion University (ODU), are diligently working on these analyses.

### 3.1 Timelike Compton Scattering with CLAS12

Compton scattering has long been identified as a golden process among deep exclusive reactions in the experimental study of Generalized Parton Distributions (GPDs). Deeply Virtual Compton Scattering (DVCS), the exclusive electroproduction of a real photon  $ep \rightarrow e'p'\gamma$ , proposed in Refs. [Mül+94; Ji97b; Ji97c; Rad97], has been the preferred tool for accessing GPDs, with significant data collected using 6 GeV CEBAF [Ste+01; Cam+06; Gir+08; Sed+15; Pis+15; Jo+15] and more recently with 12 GeV electron beams [Chr+23]. In the meantime, Timelike Compton Scattering (TCS) has been widely discussed theoretically [BDP02; BGV15; Nad+09; BGV16], but never measured experimentally until now.

TCS is the symmetric process of DVCS: the incoming photon is real and the outgoing photon has a large timelike virtuality. In TCS, the virtuality of the outgoing photon  $Q'^2 \equiv M^2$ , where  $M$  is the invariant mass of the lepton pair, sets the hard scale. The circularly polarized photon beam allows for measurement of the photon polarization asymmetry  $A_{\odot U}$  and the forward-backward asymmetry ( $A_{FB}$ ) in TCS [BGV15; HKV21].  $A_{\odot U}$  is proportional to the  $\sin \phi$  moment of the polarized interference cross section, which allows access to the imaginary part of the Compton Form Factors (CFFs), dominated by  $\mathcal{H}$ , and provides a pathway to test the universality of GPDs. The TCS  $A_{FB}$  projects out the  $\cos \phi$  moment of the unpolarized cross section, which is proportional to the real part of the CFF  $\mathcal{H}$  (see supplemental material of Ref. [Cha+21]), and thus gives access to the  $D$ -term in the parameterization of the GPDs.

The different RG-A datasets were calibrated and analyzed separately due to variations in beam energy and magnetic field settings. The first-ever experimental results on photon polarization and angular asymmetries in TCS, published in PRL [Cha+21], utilized the fall 2018 inbending dataset, which had the highest

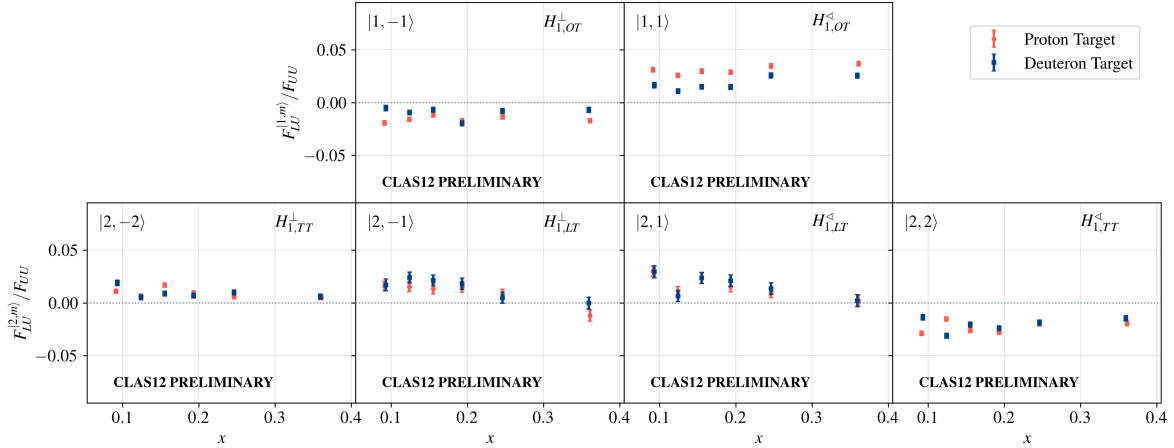
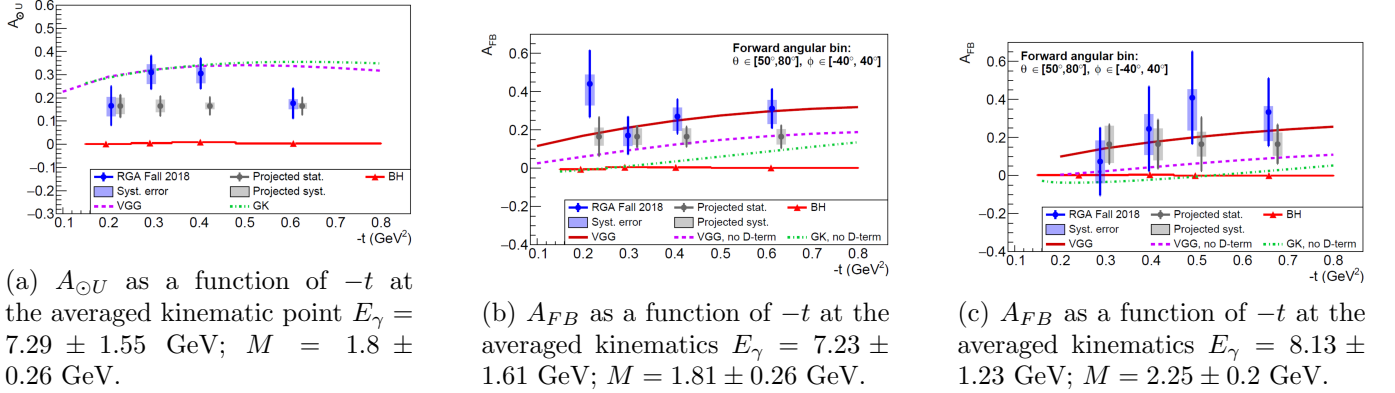
Twist-3  $F_{LU}/F_{UU}$  Amplitudes


Figure 9: Beam spin asymmetry from  $ep \rightarrow e'\pi^+\pi^-X$  (light red circles) and  $ed \rightarrow e'\pi^+\pi^-X$  (dark blue squares) in bins of Bjorken- $x$ . Each sub-figure is for a different partial wave; the sensitive  $e(x)$  and the DiFF are shown in the upper-right corners. Differences between the proton target and deuteron target results indicate a flavor-dependence of  $e(x)$ . From Ref. [Dil22].

quality calibration available at the time. A comparison of obtained results with theoretical predictions is shown in Fig. 10. The measured polarization asymmetries are in approximate agreement with the predictions obtained from models based on the GPD formalism and hence serve as an independent validation of the universality of the GPDs. The  $A_{FB}$  asymmetry, which constitutes the first direct measurement of the real part of CFFs through TCS, is better described by the model when the  $D$ -term is included in the calculations.



(a)  $A_{OU}$  as a function of  $-t$  at the averaged kinematic point  $E_\gamma = 7.29 \pm 1.55$  GeV;  $M = 1.8 \pm 0.26$  GeV.

(b)  $A_{FB}$  as a function of  $-t$  at the averaged kinematics  $E_\gamma = 7.23 \pm 1.61$  GeV;  $M = 1.81 \pm 0.26$  GeV.

(c)  $A_{FB}$  as a function of  $-t$  at the averaged kinematics  $E_\gamma = 8.13 \pm 1.23$  GeV;  $M = 2.25 \pm 0.2$  GeV.

Figure 10: Polarization (10a) and forward-backward (10b and 10c) asymmetries (in blue) and their comparison with theoretical models reported in [Cha+21]. The gray points (not in the original paper) represent the expected uncertainties when all collected data F18 and S19 are analyzed with improved reconstruction software currently available. See the original paper for a detailed description of points and curves.

Besides these qualitative conclusions, TCS is expected to contribute further to the ongoing efforts to extract GPDs from the experimental observables. Precision measurements in small kinematic bins are required to meaningfully impact the global fits to extract GPDs from the data.

Since the publication in PRL, notable advancements in the reconstruction efficiency of charged particles in CLAS12 have been achieved, particularly with the adoption of Artificial Intelligence (AI)-based tools [Gav+22]. In the case of a three-charged track final state (as in the case of TCS and  $J/\psi$  production),

the improvement of reconstruction efficiency is up to a factor of two (kinematics dependent). We recently estimated the expected statistical uncertainties of the TCS asymmetries when all the data on hand are combined. The entire available data will reduce uncertainties by half for the same data binning as shown in Fig. 10 with the gray data points.

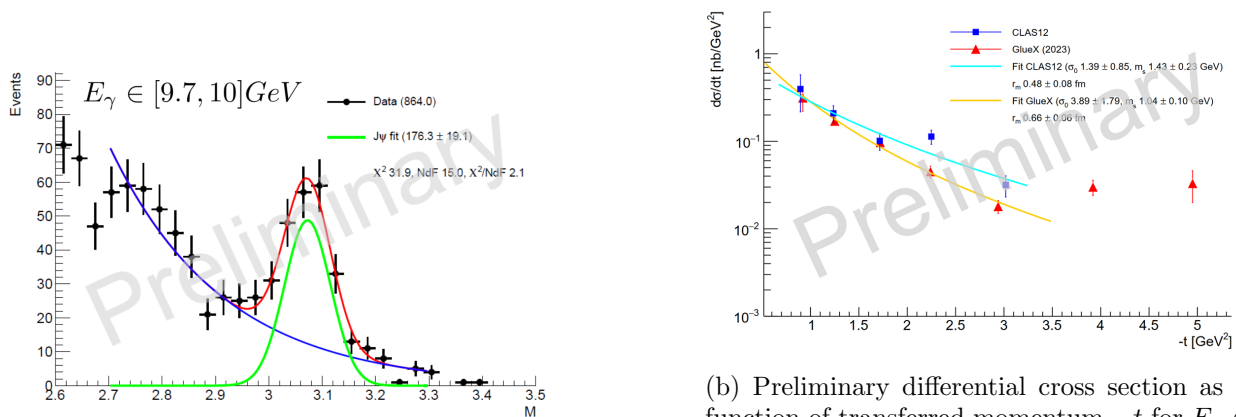
However, to fulfill the objective of analyzing data in finely segmented kinematic bins in  $Q'^2$  and total CM energy  $s$ , it remains crucial to collect all the remaining data of RG-A. Studies of dependencies of the TCS asymmetries on  $Q'^2$  and  $s$  provide powerful constraints for the extraction of the GPDs. A high-precision measurement of the TCS forward-backward asymmetry will not only be indispensable for global GPD fits, but it will also deliver valuable input to the current efforts on the extraction of the proton Gravitational Form Factors (GFFs) [BEG18; Bur+23; HPS23].

### 3.2 $J/\psi$ Photoproduction with CLAS12

The electron elastic scattering experiments were crucial in discovering that the proton has a finite size (Hofstadter's experiment in the 1950s [HFM53; HM55]) and exploring the charge and current distributions inside the nucleon (electric and magnetic form factors). These experiments also played an important role in the precise determination of the proton charge radius (as an example, one of the most recent measurements carried out in Hall B is Ref. [Xio+19]).

However, electron elastic scattering cannot probe the mass distributions inside the proton, as most of the nucleon's mass is generated by the internal dynamics of gluons. Recent developments in this field suggest that the gluon GFFs of the proton can be accessed through the photoproduction of the  $J/\psi$  meson near its production threshold. In particular, the  $t$ -dependence of the differential cross section is directly sensitive to the mass-radius of the proton [Kha21].

The aim of the studies of the  $J/\psi$  photoproduction near the energy threshold is to explore the proton's GFFs and its mass-radius. This experiment's goal is to measure the differential cross section as a function of transferred momentum  $-t$  and study its behavior as a function of incoming photon energy.



(a)  $e^-e^+$  pair invariant mass distribution and the fit around the  $J/\psi$  mass in one of the photon energy bins.

(b) Preliminary differential cross section as a function of transferred momentum  $-t$  for  $E_\gamma \in [8.2, 9.28]$  GeV. Blue squares represent CLAS12 data. Red squares represent the results obtained by the GlueX Collaboration [Adh+23a].

Figure 11:  $e^-e^+$  pair invariant mass distribution in one of the photon energy bins (left) and preliminary fitted differential cross section in the  $E_\gamma \in [8.2, 9.28]$  GeV bin (right).

Recently, two experiments conducted at Jefferson Lab, one in Hall-C (E12-16-007) and one by the GlueX Collaboration, released their results on the  $J/\psi$  differential cross sections near threshold, including their respective extraction of the mass-radius of the proton [Dur+23; Adh+23a]. Our first analysis of  $J/\psi$  photoproduction near threshold using the RG-A datasets will be finalized and released by fall 2024.

Figure 11 shows the  $e^-e^+$  pair invariant mass distribution in one of the photon energy bins (Fig. 11a) and the preliminary differential cross section in the  $E_\gamma \in [8.2, 9.28]$  GeV bin (Fig. 11b). The  $t$ -dependence is fitted with a dipole function to extract the proton mass radius (Fig. 11b). The uncertainties obtained with the CLAS12 dataset in this given energy bin are comparable to the ones reported by the GlueX Collaboration. However, we do not have sufficient statistics at larger  $-t$ , where GlueX reports a flattening behavior of the cross section. Collecting the remaining portion of the RG-A data will allow us to reduce the current statistical uncertainties and reach the higher  $-t$  region to verify the behavior observed by the GlueX Collaboration independently.

### 3.3 Summary

Since the completion of the RG-A runs in 2018 and 2019, the CLAS Collaboration has made significant progress in data calibration, reconstruction efficiency, and analysis. The very first experimental measurement of TCS asymmetries based on the fraction of the obtained data was published in PRL in 2021, with the comprehensive analysis of the  $J/\psi$  cross section nearing completion. The published results on TCS and the one on  $J/\psi$ , which will be released soon, are significant. The TCS results suggest the universality of GPDs and the importance of the  $D$ -term in the parameterizations of the GPDs. At the same time,  $J/\psi$  cross section results will allow us to understand the gluon distribution in the nucleon and extract its mass radius. Nevertheless, many critical points remain to be addressed, such as reaching a more quantitative conclusion in the parameterizations of GPDs, increasing the accuracy of the  $J/\psi$  cross section measurements, and covering the higher  $-t$  region. Collecting the remaining part of the RG-A data appears paramount to fulfill these objectives.

## 4 Hadron Structure Experiments (E12-06-108A and E12-09-113)

### 4.1 Physics Motivation

Studies of the structure of excited nucleon states in terms of the  $Q^2$ -evolution of their  $\gamma_v p N^*$  electrocouplings represent the only source of information on many aspects of the emergence of strong QCD underlying the generation of  $N^*$  states of different quantum numbers [MC22; Gro+23]. Continuum-QCD approaches (CSM) and most available quark models reproduce the nucleon elastic form factors equally well but predict different behaviors for the  $\gamma_v p N^*$  electrocouplings. Confronting theory expectations with the data will allow us to shed light on how resonances of different structures emerge from QCD. The  $\gamma_v p N^*$  electrocouplings are also of particular importance for gaining insight into the strong QCD dynamics responsible for the emergence of hadron mass (EHM). Recent advances in CSM approaches make it possible to connect the EHM dynamics expressed in terms of the momentum dependence of the QCD-running coupling and the dressed quark and gluon masses with the  $Q^2$ -evolution of the  $\gamma_v p N^*$  electrocouplings [Car+23; DRS23].

Together, the approved experiments E12-09-003 and E12-06-108A are the cornerstones of the CLAS12 program  $N^*$  and will allow us to investigate the range of  $Q^2$  that overlaps the existing CLAS data and to significantly extend the coverage of the data up to 10-12 GeV<sup>2</sup>. In this kinematic range, the reactions probe distances where around 50% of hadron mass is expected to emerge in the transition between the strongly coupled and pQCD regimes, addressing the key open question of the Standard Model on the emergence of hadron mass and  $N^*$  structure. Consistent results on the  $\gamma_v p N^*$  electrocouplings from the  $\pi N$ ,  $\eta N$ ,  $\pi\pi N$ , and  $KY$  electroproduction channels with different non-resonant contributions will further validate the reliable and controlled extraction of these quantities.

### 4.2 Status of Current Analysis Studies

The data analysis related to E12-09-003 and E12-06-108A on the fall 2018 and spring 2019 datasets is being carried out by teams at Jefferson Lab, the University of South Carolina, Moscow State University,

James Madison University, and the University of Connecticut under the aegis of the CLAS12 Hadron Structure Group. The existing data analysis for both experiments has focused on isolating the reaction channels in their different topologies, momentum corrections to optimize the resolution, yield extractions, and detailed comparisons of the event distributions to the CLAS12 Geant4 Monte Carlo using data-based event generators. These analyses have advanced significantly on two fronts. The first is the extraction of the inclusive electron scattering cross section in the resonance region from the RG-A data for fall 2018 that spans  $Q^2$  up to  $10 \text{ GeV}^2$ . The preliminary results suggest promising opportunities for the extraction of the  $\gamma_v p N^*$  electrocouplings from exclusive meson electroproduction data as resonance structures are clearly seen in the second and third resonance regions over the full  $Q^2$  range (see Fig. 12). Using a framework for the evaluation of the resonant contributions based on the CLAS results for the  $N^*$  electroexcitation amplitudes, estimates for the resonant contributions to inclusive electron scattering have been determined [HMM23; Hil+19; Hil+21]. These results pave the way for insight into the nucleon-parton distributions in the resonance region and will extend our understanding of quark-hadron duality. This first cross section analysis from CLAS12 is now under review within the CLAS Collaboration. The second advanced analysis from the RG-A dataset based on the fall 2018 run is the exclusive analysis of the  $\pi^+ \pi^- p$  final state. The extraction of the  $\pi^+ \pi^- p$  cross sections will be completed in the next year. This measurement will allow us to determine  $\gamma_v p N^*$  electrocouplings within the limited  $Q^2$  range up to  $5\text{--}6 \text{ GeV}^2$  due to the limited statistics of the data collected currently (see Fig. 13). The remaining approved RG-A beam time will be necessary to extend the cross sections up to  $10 \text{ GeV}^2$ . This remaining data is especially important given the issues with the spring 2018 data.

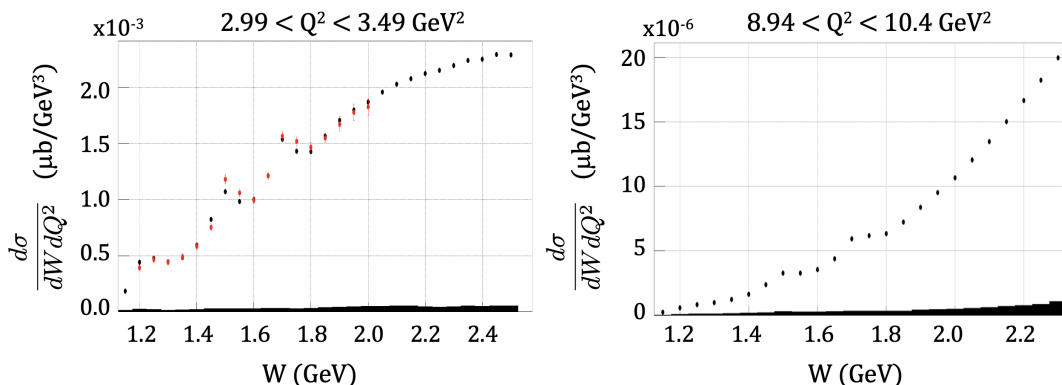


Figure 12: Preliminary inclusive electron scattering cross sections from the RG-A fall 2018 data in black for two  $Q^2$ -bins from  $3.0\text{--}3.5 \text{ GeV}^2$  in comparison with interpolated world data in red (left) and from  $8.94\text{--}10.4 \text{ GeV}^2$  (right).

Due to the limitations of the operating conditions of the forward drift chambers during the RG-A runs, the missing mass resolution is not sufficient to adequately separate the  $\Lambda$  and  $\Sigma^0$  final states (see Fig. 14). Starting in 2020, the drift chamber systems were upgraded to enable significant improvements in the charged particle momentum resolution. This improvement has also been accompanied by improved precision in the detector alignment technique, the calibration algorithm, and the reconstruction approach for forward charged particle tracking. These together have enabled nearly a factor of two improvement in the forward tracking momentum resolution. Thus, future RG-A data collection is an absolute requirement for a viable  $KY$  electroproduction program with CLAS12 at  $11 \text{ GeV}$  to deliver on the promises of E12-06-108A.

### 4.3 Projections for Remaining Data Collection

The fall 2018 and spring 2019 RG-A datasets amount to less than 30% of the full approved RG-A beam time. The yields from the  $\pi N$ ,  $\pi\pi N$ , and  $KY$  channels from the fall 2018 data in the kinematic range up to  $Q^2 = 5 \text{ GeV}^2$  in the resonance region are essentially equivalent to what has already been measured and

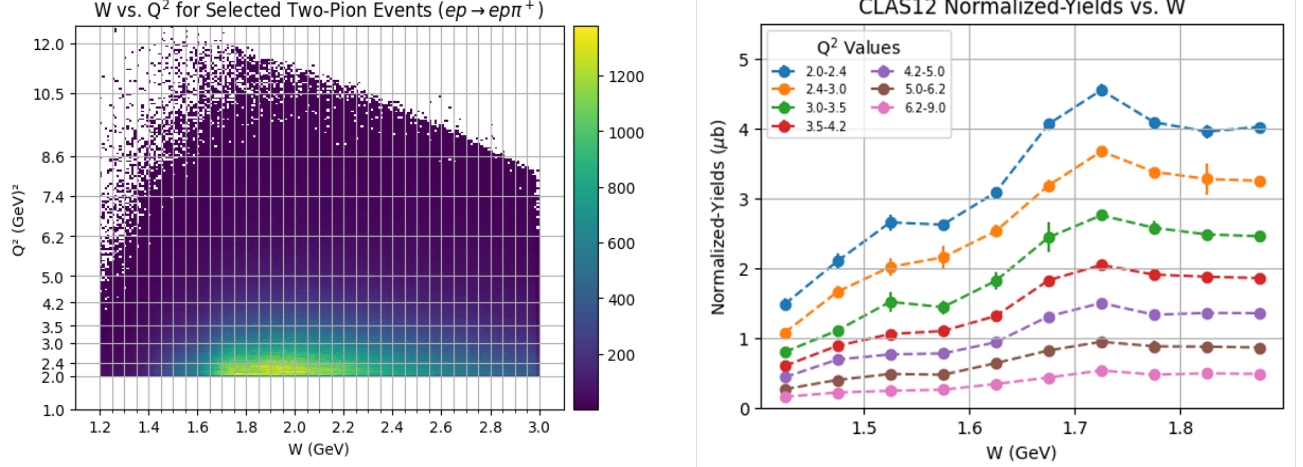


Figure 13: (Left) Preliminary measured yields based on the RG-A fall 2018 data for each  $W$  and  $Q^2$  bin in which nine single-differential  $\pi^+\pi^-p$  cross sections are to be determined. (Right) Preliminary normalized yields in the dependence of  $W$  for each  $Q^2$  bin.

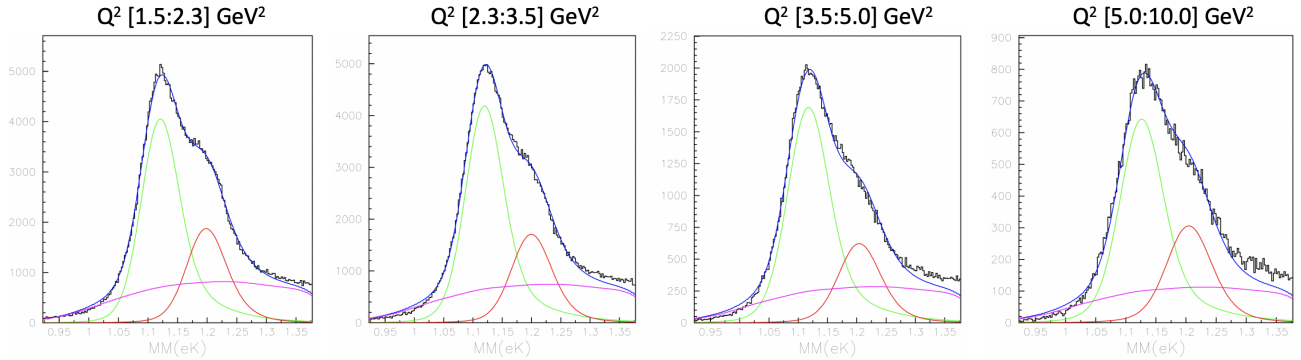


Figure 14:  $MM(e'K^+)$  spectra (GeV) from the RG-A fall 2018 data from the  $e'K^+p$  topology for four different bins in  $Q^2$  spanning the CLAS12 acceptance. The fitting function separates the contributions from  $K^+\Lambda$ ,  $K^+\Sigma^0$ , and background.

published from CLAS in these different channels. However, the primary emphases of the two approved RG-A hadron structure experiments are 1) to provide for more than an order of magnitude increase in statistics for the different final states compared to the data available from CLAS and 2) to significantly extend the kinematic range of the available data to the essentially unexplored region of  $Q^2$  up to 10-12  $\text{GeV}^2$ . In order to realize the experiment goals of the  $N^*$  program with CLAS12, it is imperative that the PAC approves the remainder of the RG-A beam time. Relying only on the RG-A data collected to date will not allow for the significant extension in  $Q^2$  promised by the CLAS12 12-GeV upgrade and will not allow for a viable  $KY$  program at 11 GeV.

## 5 MesonEx Physics (E12-11-005)

### 5.1 Introduction

Understanding quark and gluon confinement in QCD is one of the outstanding issues in physics. To this end, hadron spectroscopy is a powerful tool for investigating how the QCD partons manifest themselves under the strong interaction at the energy scale of the nucleon mass (GeV). The experiment (E12-11-005 or MesonEx) aims to study the meson spectrum, searching for exotic states, with precise determination of resonance

masses and properties with a high-statistics and high-resolution experiment. The CLAS12 spectrometer augmented by the Forward Tagger (FT) allows electron scattering at very low  $Q^2$  ( $10^{-2} - 10^{-1}$  GeV<sup>2</sup>), which provides a high photon flux and a high degree of linear and circular polarization, complementary to the capabilities of Hall D, and providing the potential to cross-check results. The quantum numbers of meson resonances are defined via partial wave analysis (PWA) of their decay products. The partial waves may be extracted from the resonance decay distributions through sophisticated amplitude analysis fitting methods. Experimentally, this requires datasets with sufficient statistics and accurate modeling of detector and reconstruction responses to allow precise acceptance corrections.

## 5.2 Physics Overview

Recently, significant progress has occurred in understanding the meson spectrum. In the charmonium sector many candidates for exotic mesons have been discovered, but the nature of these states is not well understood. Explicit measurement of exotic partial waves, a goal of MesonEx, still remains one of the cleanest methods to identify true hybrid states (containing constituent gluons). The worldwide interest in exotic hybrids is shown by recent publications of the COMPASS Collaboration at CERN reporting results on the final states  $\eta\pi$ ,  $\eta'\pi$  and  $3\pi$  [Ado+15; Agh+18]. Structures compatible with hybrid mesons with quantum numbers  $J^{PC} = 1^{-+}$  are clearly identified. MesonEx, via photoproduction of mesons as opposed to pion production, is vital to validate these results while extending searches outside the isovector sector.

The theoretical analysis reported in Ref. [Rod+19] permitted the identification of the seemingly different peaks in  $\eta\pi$  and  $\eta'\pi$  seen in the COMPASS data [Agh+18] as a single  $\pi_1(1600)$  state, in agreement with QCD expectations [Dud11; SK06]. In addition to these studies, MesonEx has the potential to understand the microscopic structure of hybrids by measuring the coupling to photons [GYS14].

A comprehensive understanding of the dynamics of meson production is needed to pin down the properties of new resonances. In particular, the mechanisms dominating ordinary meson production must be identified first. Studies of single meson production have been shown in Refs. [MFS15; Nys+18; Mat+20] and provide predictions for (un)polarized cross sections at CLAS12.

Another topic of great interest concerns the lightest scalar meson multiplet [PR20; Bri+17; Wil+19]. The heavier isoscalar scalars are poorly understood. In the PDG, three  $f_0$  states are reported below 2 GeV. This is one more than the quark model expectations, suggesting a contribution from a glueball [Gia+05; KZ07]. However, the existence of three different states is not compelling as they do not appear together in the same reaction. Data from MesonEx in  $\pi\pi$  and  $KK$  photoproduction can solve the controversy. The last few years have seen new studies to best represent amplitudes with multi-body final states. This is crucial when resonances in different channels interfere [Pil+18; Mik+20], and in the context of MesonEx is needed to properly take into account contamination from baryon resonances [Pau+18].

Concerning this proposal, notable activities in amplitude analysis carried by the Joint Physics Analysis Center (JPAC) enhance the reliability and interpretation of the prospective results. In collaboration with MesonEx, JPAC is providing new tools to extract robust physics information from CLAS12 data. JPAC has constructed observables sensitive to the presence of mesons with exotic quantum numbers that can be measured by MesonEx with sufficient statistics [Mat+19]. Further detailed studies have recently been performed confirming polarized photoproduction as an effective tool for partial wave analysis [Smi+23].

Looking ahead the EIC will try and hunt for exotic charmonium states via the same production mechanism, quasi-real photoproduction. Detailed measurements by MesonEx will increase our knowledge of spectroscopy with electron beams and benefit this future enterprise.

## 5.3 Assessment and Future Plans

A broad investigation of different channels was carried out with the CLAS12 RG-A pass-1 reconstruction data. Three Ph.D.s were subsequently awarded at User Institutions.

- Matthew Nicol, University of York, “Exploring the strong interaction through electroproduction of exotic particles”, 2023
- Letterio Biondi, University of Messina, “Investigation on exclusive beam asymmetry measurements of  $e + p \rightarrow e + p + \pi^0$  process at CLAS12” , 2023
- Robert Wishart, University of Glasgow, “Analysis of three body decays in quasi-real photoproduction”, 2023

The results from these first analyses showed that the preliminary reconstruction of CLAS12 was able to provide decay distributions for partial wave analysis. However for detailed and reliable results, further work was needed to increase the reconstruction efficiency and better understand the acceptance. The CLAS Collaboration has since performed significant optimizations towards this end, and new data were released at the end of 2023. These data are now undergoing analysis but it is clear resolutions and efficiencies are much improved, by a factor of 2 in the latter case, which will be sufficient for our analyses.

As a benchmark, we are analyzing the decay of  $\rho$  to  $\pi^+\pi^-$ . The Spin Density Matrix Elements were recently published by GlueX as their first analysis of meson decay distributions [Adh+23b]. In CLAS12 kinematics, these same decays should have very similar distributions. The GlueX results showed that  $s$ -channel helicity conservation is applicable and the partial waves should be dominated by the positive reflectivity  $P_+$  wave. In Fig. 15, we show preliminary partial waves in the  $\rho$  mass region as a function of the four-momentum transfer squared for the spring 2019 dataset. Although these results are very preliminary, the basic trends are what we would expect with small  $s$ -wave and negative reflectivity contributions. In addition, this analysis takes advantage of the combined linear and circular polarization available with quasi-real photoproduction with the Forward Tagger, providing cleaner results than with linear polarization alone.

In order to extract the partial waves with minimum biases we are currently exploring generative machine learning techniques and led a pilot study using such procedures on a two pion photoproduction to unfold resolution effects in the reaction reconstruction [Alg+23].

The primary channel for MesonEx is still expected to be the three-charged-pion charge-exchange reaction. As mentioned earlier, the COMPASS results found a strong exotic signal in this final state and it is important to reproduce this with an alternative production mechanism. The amplitude analysis for this reaction is significantly more complicated than for two-body (or quasi-two-body) final states and the plan is to first determine reliable amplitudes from the simpler reactions  $\pi^+\pi^-$ ,  $K^+K^-$ , and  $K^*K^+$  as shown for the  $\rho$  earlier.

We can, however, see from the multi-dimensional mass plots in Fig. 16 the intermediate decay channels for  $2\pi^+\pi^-$  expected and outlined in the original proposal. This includes peaks in the  $3\pi$  mass at the  $a_2(1320)$  and in the intermediate  $2\pi$  mass at the  $\rho$  and  $f_2(1270)$ . For the spring 2018 dataset, we currently have 3.7M  $3\pi$  events reconstructed for these plots.

## 5.4 Summary

MesonEx requires finding small exotic signals in reactions dominated by conventional mesons. The reliability of the results depends critically on having sufficient statistics to disentangle the smallest contributions. The RG-A datasets with full statistics will provide millions of events for this analysis. For some lower cross section reactions, such as  $K^*K$  that can contain exotic waves, running the full beam time is imperative. Our understanding of Partial Wave Analysis with polarized photoproduction continues to improve and through collaboration with the larger community and MesonEx, with its combined linear and circular polarization, is well placed to capitalize on this. The significant progress made in data reconstruction, calibration, and trigger (from the original RG-A), will result in new beam times with an extended and optimized dataset for the rarer channels such as multi-neutral or multi-kaon exclusive states.

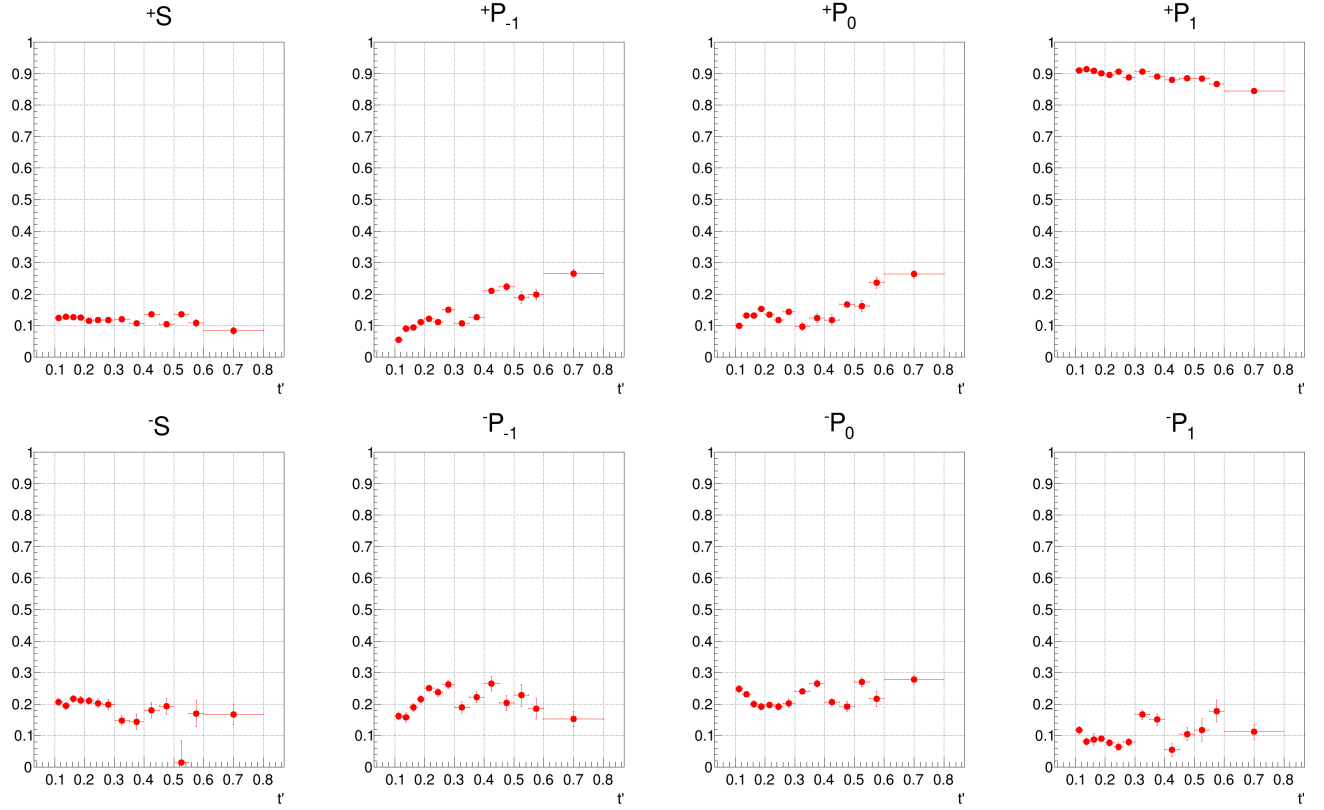


Figure 15: MesonEx Partial Wave Amplitudes extracted for the  $\rho$  as a function of four-momentum transfer squared. The top row shows the positive reflectivity amplitudes, (*i.e.*, natural parity exchange), the bottom negative.

## 6 VeryStrange Physics (E12–11–005a)

### 6.1 Introduction

Experiment E12–11–005 or VeryStrange aims to study the electroproduction and photoproduction of the  $S = -2, -3$  baryons in exclusive reactions with the CLAS12 detector. The data will be used to find new and missing excited states  $\Xi$ , possibly measuring their quantum numbers and the mass splitting of the ground state and excited doublets  $\Xi$ . These data samples will also provide the statistics necessary for measuring, for the first time as a function of kinematic variables, the beam polarization transfer and induced polarization of the ground state  $\Xi^-$  in the reaction  $\gamma p \rightarrow \Xi K^+ K^-$ . The  $\Omega^-$  has not yet been seen in electro- or photoproduction. The distinctive feature of this process is that none of the three constituent  $s$  quarks in  $\Omega^-$  come from the target nucleon. The only available data [Abe+85] set an upper limit of the photoproduction cross section of  $\Omega^-$ .

### 6.2 Science Update

As far as the strangeness sector is concerned, very few new data were published since the original proposal and the study of the spectrum of very strange baryons remains compelling. Recent results from the BELLE Collaboration on  $\Xi^- \pi^+$  spectra are very interesting, particularly for the evidence of the  $\Xi(1620)$  [Sum+19a]. CLAS results on the  $\Xi(1530)$  cross section from a similar channel ( $\Xi^0 \pi^-$ ) published in 2007 [Guo+07] did report a bump around 1620 MeV (although not statistically significant). Still, after the recent BELLE observation [Sum+19b] and pole position determination [NH24], it became attractive. The VeryStrange physics program is still of high interest, with a unique opportunity to provide results in unexplored territo-

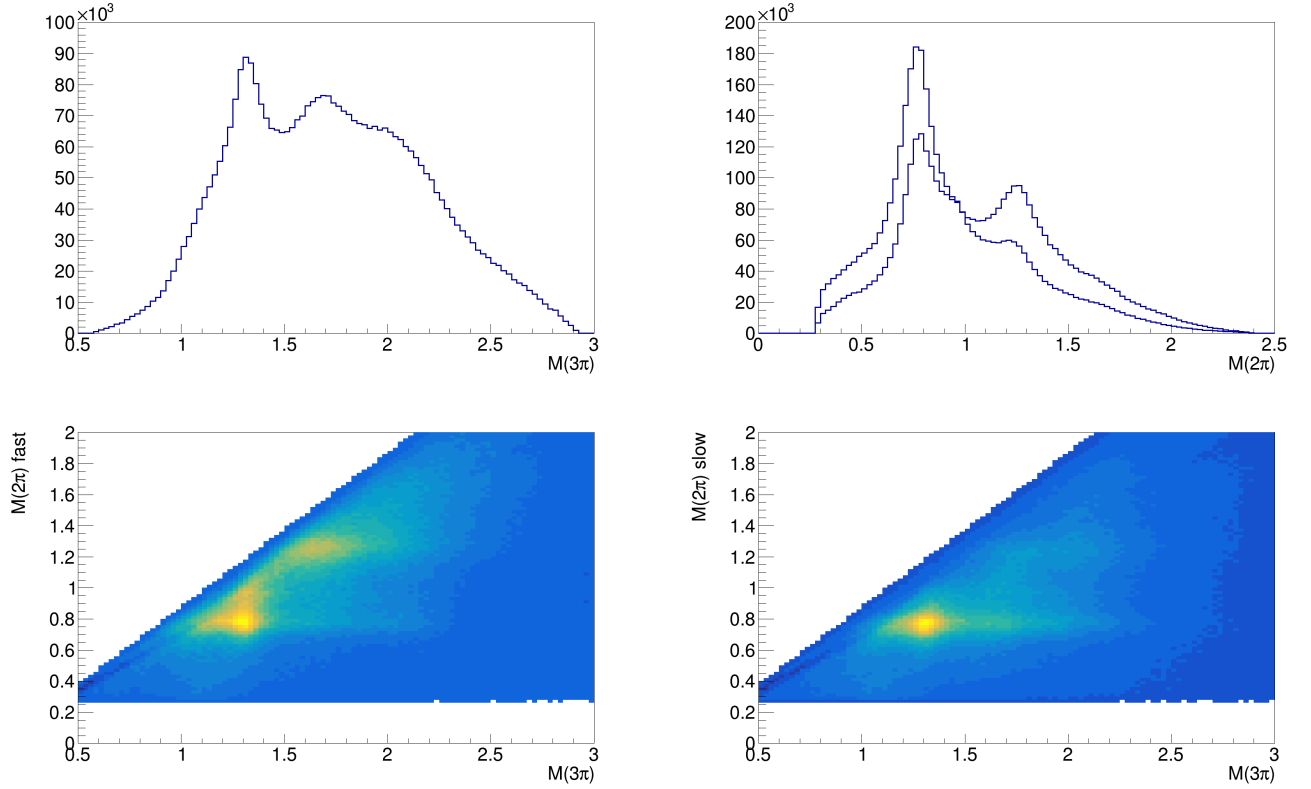


Figure 16: Mass distributions for the three pion reaction.

ries: Any results of  $\Xi$  electroproduction would be new, whether detailed differential cross sections or total cross sections will be measured. The  $Q^2$  dependence can provide us with new valuable and complementary information on these states that no facility other than JLab can obtain. The complementary of electroproduction versus photoproduction in the search for missing resonances has recently been illustrated [Mok+20]. The nonresonant background has a strong  $Q^2$  dependence and is negligible at the largest  $Q^2$ . The ground state hyperons ( $S = -1$ ) are very well known. However, there are remarkably few precision data on excited hyperon states. The electroproduction of  $\Lambda(1405)$  is particularly important. The nature of this state is still not clearly understood (see, for instance, [Sad+23]). The study of the  $Q^2$  dependence of its cross section can help to solve this puzzle. With a full statistics dataset, RG-A is poised to make major contributions to the spectroscopy of excited hyperons. This is particularly timely in the new era of precision Lattice QCD calculations.

### 6.3 Assessment and Future Plans

The VeryStrange experiment will clearly benefit from collecting the remaining statistics. For the VeryStrange program, we expect sufficient statistics for ground-state cascades and excited  $S=-1$  hyperons. But excited cascades and  $\Omega^-$  would need as much statistics as we can get. For the existing RG-A data using a beam charge of about 250 mC, we have obtained first-time measurements of electroproduction cross sections for the ground state cascade. The missing mass spectra of  $eK^+K^+$  can be seen in Fig. 17. The ground state  $\Xi^-(1320)$ , as well as  $\Xi^-(1530)$ , are clearly identifiable using electrons detected in the Forward Tagger (left) and the Forward Detector (right). Both spectra show a clear excess of events in the region around 1.8–2.0 GeV. However, with the available statistics, it is not feasible to clearly identify and separate potential multiple states in the region. Statistically, these are consistent with our expectation of about 300  $\Xi(1820)$ s using the upper limit of cross section from the CLAS g12 results [Goe18] and consistent with the GlueX

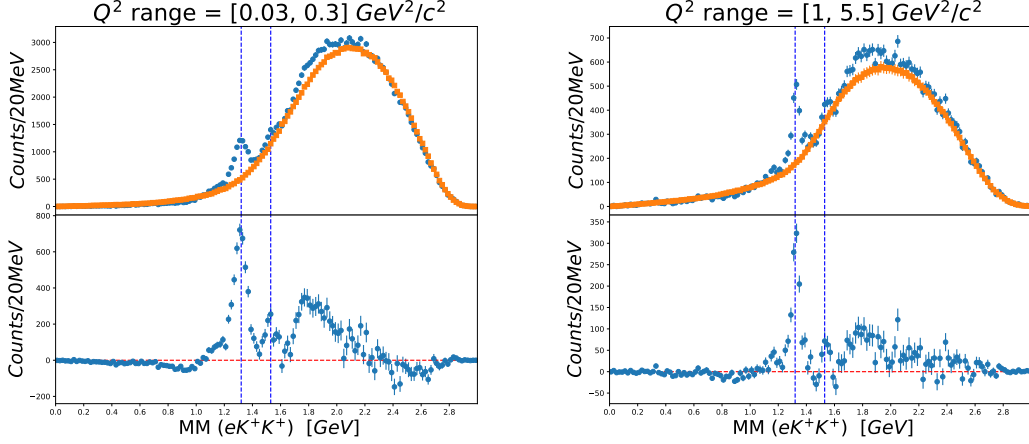


Figure 17: Preliminary  $eK^+K^+$  missing mass spectra using the CLAS12 RG-A dataset (spring 2019) in the reaction of  $ep \rightarrow e'K^+K^+(X)$  with the electron beam energy of 10.6 GeV; Left: The electrons are detected in the Forward Tagger. Right: The electrons are detected in the Forward Detector. A background of mixed events (filled) is normalized to the data outside the signal region (1.2 – 2.0 GeV). The bottom spectra are obtained by subtracting the mixed-event background. The two vertical lines indicate the nominal masses of  $\Xi^-(1320)$  and  $\Xi^-(1530)$ .

results. In addition, the excited cascades have also been studied via their  $K^-\Lambda$  and  $K^-\Sigma$  decay channels, using the reaction of  $ep \rightarrow e'K^+K^+K^-(X)$ . The hyperons can be seen in the missing mass spectra when all three kaons are identified in the CLAS12 Forward Detector. However, due to the low statistics in the existing RG-A data, only an upper limit of the excited cascade cross section has been obtained. Considering the lower cross section and the lower virtual photon flux at finite  $Q^2$ , the electroproduction part of the VeryStrange proposal can only be studied by accumulating the full assigned statistics. We stress that these measurements of excited cascades would be the first of their kind, suggesting a contribution from a glueball [Gia+05; KZ07]. The VeryStrange program is also complementary to the KLF at Hall D program C12-19-001 [Ama+20] to look for missed hyperons.

A search for  $\Omega^-$  in the reaction  $ep \rightarrow e'\Lambda K^-(X)$ , where the candidate  $\Lambda$  is reconstructed its  $p\pi^-$  decay was done using the RG-A fall 2018 and spring 2019 datasets. The  $\Omega^-$  candidate is reconstructed in the  $\Omega^- \rightarrow \Lambda K^-$  decay. Events with at least one electron, one proton, and one  $K^-$  are skimmed. An algorithm that estimates the position of the  $\Lambda$  hyperon detached vertex is used to improve the signal-to-background ratio. The reconstructed  $m((p\pi^-)K^-)$  mass obtained after selecting the  $\Lambda \rightarrow p\pi^-$  signal is shown in Fig. 18 (left).

Strangeness conservation dictates that expected events should have at least two positively charged kaons and a neutral kaon so that the missing mass against the reconstructed electron, proton,  $\pi^-$ , and  $K^-$  (MM) should exceed 1.35 GeV. This value is the minimum (within resolution) missing mass threshold for  $\Omega^-$  production. The  $\Xi^-(1690)$  resonance also decays to  $\Lambda K^-$ . This results in a possible ambiguity for an observed signal in the region of the expected  $\Omega^-$ . However, the MM threshold (0.85 GeV) for doubly strange  $\Xi^-(1690)$  is lower than that for  $\Omega^-$ , and the  $m((p\pi^-)K^-)$  spectra corresponding to their respected expected production thresholds can be compared to study possible contamination from  $\Xi^-(1690)$  to the peak  $\Omega^-$ , as shown in Fig. 18 (right).

With the datasets used in this analysis, a statistical significance close to 3 standard deviations is obtained, clearly highlighting the need for more statistics. Within the remaining approved RG-A beam time we expect to collect several times more statistics for this reaction. If the signal is confirmed, it will constitute the first observation of the  $\Omega^-$  in electroproduction.

The analysis of the data on multiple strangeness production from the first installment of RG-A resulted

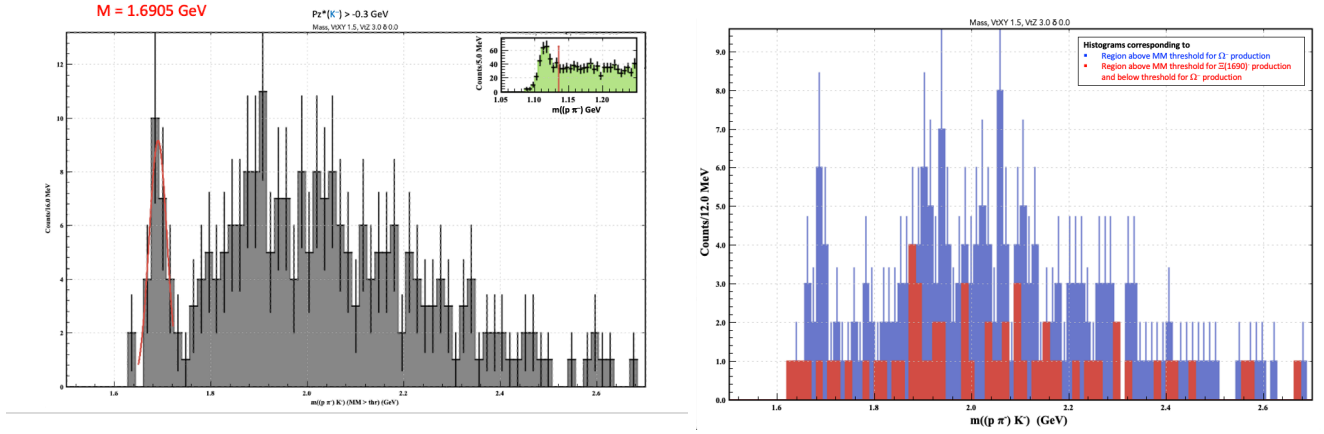


Figure 18: Reconstructed  $m((p\pi^-)K^-)$  spectrum corresponding to the  $\Lambda \rightarrow p\pi^-$  signal region (indicated by the red line in the figure upper insert). Left:  $MM > 1.3$  GeV. A center-of-mass  $z$ -momentum cut of  $p_z^*(K^-) = -0.3$  GeV is imposed on the  $K^-$ . Right:  $MM > 1.3$  GeV [blue] and for  $0.85 < MM < 1.3$  GeV [red]. (Preliminary)

in two Ph.D.s:

- Achyut Khanal, *Search for Excited Cascade Hyperons  $\Xi^{*-}$  Using the CLAS12 Spectrometer at Jefferson Laboratory*, 2022
- Jose Carvajal, *First Time Measurement of Ground-State  $\Xi^-$  Hyperon Cross-Section in Electroproduction*, 2024.

## 7 Summary

The RG-A science program is robust and diverse, delving into key inquiries in hadronic physics. CLAS12 has not only met, but surpassed design specifications in some cases. A sophisticated smart trigger has been developed to manage the 13 experiments simultaneously, optimizing performance. Advanced calibration, processing, and analysis of half of the RG-A data are underway across all programs, with initial publications already out. However, to fully unlock the program’s potential for scientific breakthroughs, complete access to the approved beam time is imperative. This will leverage the extended  $Q^2$  capabilities promised by the CLAS12 12-GeV upgrade, promoting opportunities for discovery potential.

## References

- [BR05] A. V. Belitsky and A. V. Radyushkin. In: *Phys. Rept.* 418 (2005), pp. 1–387.
- [Die03] M. Diehl. In: *Phys. Rept.* 388 (2003), pp. 41–277.
- [KLM16] K. Kumericki, S. Liuti, and H. Moutarde. In: *Eur. Phys. J. A* 52.6 (2016), p. 157.
- [PS18] M. V. Polyakov and P. Schweitzer. In: *Int. J. Mod. Phys. A* 33.26 (2018), p. 1830025.
- [Bur18] V. D. Burkert. In: *Ann. Rev. Nucl. Part. Sci.* 68 (2018), pp. 405–428.
- [BM10] A. V. Belitsky and D. Mueller. In: *Phys. Rev.* D82 (2010), p. 074010.
- [AGL09] S. Ahmad, G. R. Goldstein, and S. Liuti. In: *Phys. Rev.* D79 (2009), p. 054014.
- [Bur00] Matthias Burkardt. “Impact parameter dependent parton distributions and off forward parton distributions for  $\zeta \rightarrow 0$ ”. In: *Phys. Rev. D* 62 (2000). [Erratum: *Phys. Rev. D* 66, 119903 (2002)], p. 071503.
- [Ji97a] Xiang-Dong Ji. “Deeply-virtual Compton scattering”. In: *Phys. Rev.* D55 (1997), pp. 7114–7125.
- [Ber+21] V. Bertone et al. “Deconvolution problem of deeply virtual Compton scattering”. In: *Phys. Rev. D* 103.11 (2021), p. 114019.
- [Ber+22] Valerio Bertone et al. “Shadow generalized parton distributions: a practical approach to the deconvolution problem of DVCS”. In: *SciPost Phys. Proc.* 8 (2022), p. 107.
- [Cha+22] José Manuel Morgado Chavez et al. “Pion generalized parton distributions: A path toward phenomenology”. In: *Phys. Rev. D* 105.9 (2022), p. 094012.
- [ADL08] Daniela Amrath, Markus Diehl, and Jean-Philippe Lansberg. “Deeply virtual Compton scattering on a virtual pion target”. In: *Eur. Phys. J. C* 58 (2008), pp. 179–192.
- [Bac+07] Alessandro Bacchetta et al. “Semi-inclusive deep inelastic scattering at small transverse momentum”. In: *JHEP* 02 (2007), p. 093.
- [Kot95] Aram Kotzinian. “New quark distributions and semiinclusive electroproduction on the polarized nucleons”. In: *Nucl. Phys.* B441 (1995), pp. 234–248.
- [MT96] P. J. Mulders and R. D. Tangerman. “The complete tree-level result up to order  $1/Q$  for polarized deep-inelastic lepton production”. In: *Nucl. Phys.* B461 (1996), pp. 197–237.
- [Hay+21] T. B. Hayward et al. “Observation of Beam Spin Asymmetries in the Process  $ep \rightarrow e'\pi^+\pi^-X$  with CLAS12”. In: *Phys. Rev. Lett.* 126 (2021), p. 152501.
- [Cou+22] Aurore Courtoy et al. “Extraction of the higher-twist parton distribution  $e(x)$  from CLAS data”. In: *Phys. Rev. D* 106.1 (2022), p. 014027.
- [Dil22] Christopher Dilks. In: *Transversity 2022* (2022). URL: <https://agenda.infn.it/event/19219/contributions/170922/>.
- [Bur+20] V. D. Burkert et al. “The CLAS12 Spectrometer at Jefferson Laboratory”. In: *Nucl. Instrum. Meth. A* 959 (2020), p. 163419.
- [Mül+94] Dieter Müller et al. “Wave functions, evolution equations and evolution kernels from light ray operators of QCD”. In: *Fortsch. Phys.* 42 (1994), pp. 101–141.
- [Ji97b] Xiangdong Ji. “Deeply virtual Compton scattering”. In: *Phys. Rev. D* 55 (11 1997), pp. 7114–7125.
- [Ji97c] Xiangdong Ji. “Gauge-Invariant Decomposition of Nucleon Spin”. In: *Phys. Rev. Lett.* 78 (4 1997), pp. 610–613.

- [Rad97] A. V. Radyushkin. “Nonforward parton distributions”. In: *Phys. Rev. D* 56 (9 1997), pp. 5524–5557.
- [Ste+01] S. Stepanyan et al. “Observation of Exclusive Deeply Virtual Compton Scattering in Polarized Electron Beam Asymmetry Measurements”. In: *Phys. Rev. Lett.* 87 (18 2001), p. 182002.
- [Cam+06] C. Muñoz Camacho et al. “Scaling Tests of the Cross Section for Deeply Virtual Compton Scattering”. In: *Phys. Rev. Lett.* 97 (26 2006), p. 262002.
- [Gir+08] F. X. Girod et al. “Measurement of Deeply Virtual Compton Scattering Beam-Spin Asymmetries”. In: *Phys. Rev. Lett.* 100 (16 2008), p. 162002.
- [Sed+15] E. Seder et al. “Longitudinal Target-Spin Asymmetries for Deeply Virtual Compton Scattering”. In: *Phys. Rev. Lett.* 114 (3 2015), p. 032001.
- [Pis+15] S. Pisano et al. “Single and double spin asymmetries for deeply virtual Compton scattering measured with CLAS and a longitudinally polarized proton target”. In: *Phys. Rev. D* 91 (5 2015), p. 052014.
- [Jo+15] H. S. Jo et al. “Cross Sections for the Exclusive Photon Electroproduction on the Proton and Generalized Parton Distributions”. In: *Phys. Rev. Lett.* 115 (21 2015), p. 212003.
- [Chr+23] G. Christiaens et al. “First CLAS12 Measurement of Deeply Virtual Compton Scattering Beam-Spin Asymmetries in the Extended Valence Region”. In: *Phys. Rev. Lett.* 130.21 (2023), p. 211902.
- [BDP02] E. R. Berger, M. Diehl, and B. Pire. In: *Eur. Phys. J. C* 23 (2002), pp. 675–689.
- [BGV15] M. Boër, M. Guidal, and M. Vanderhaeghen. “Timelike Compton scattering off the proton and generalized parton distributions”. In: *Eur. Phys. J. A* 51.8 (2015), p. 103.
- [Nad+09] P. Nadel-Turonski et al. “Timelike Compton scattering: A first look”. In: *AIP Conf. Proc.* 1182.1 (2009). Ed. by Marvin L. Marshak, pp. 843–846.
- [BGV16] Marie Boër, Michel Guidal, and Marc Vanderhaeghen. “Timelike Compton scattering off the neutron”. In: *Eur. Phys. J. A* 52 (2016), p. 33.
- [HKV21] Matthias Heller, Niklas Keil, and Marc Vanderhaeghen. “Leading-order QED radiative corrections to timelike Compton scattering on the proton”. In: *Phys. Rev. D* 103 (3 2021), p. 036009.
- [Cha+21] P. Chatagnon et al. “First Measurement of Timelike Compton Scattering”. In: *Phys. Rev. Lett.* 127 (26 2021), p. 262501.
- [Gav+22] Gagik Gavalian et al. “CLAS12 Track Reconstruction with Artificial Intelligence”. In: (2022). arXiv: 2205.02616 [physics.ins-det].
- [BEG18] V.D. Burkert, L. Elouadrhiri, and F.X. Girod. In: *Nature* 557.7705 (2018), pp. 396–399.
- [Bur+23] V. D. Burkert et al. “Colloquium: Gravitational form factors of the proton”. In: *Rev. Mod. Phys.* 95 (4 2023), p. 041002.
- [HPS23] Daniel C. Hackett, Dimitra A. Pefkou, and Phiala E. Shanahan. “Gravitational form factors of the proton from lattice QCD”. In: (2023). arXiv: 2310.08484 [hep-lat].
- [HFM53] R. Hofstadter, H. R. Fechter, and J. A. McIntyre. “Scattering of High-Energy Electrons and the Method of Nuclear Recoil”. In: *Phys. Rev.* 91 (2 1953), pp. 422–423.
- [HM55] Robert Hofstadter and Robert W. McAllister. “Electron Scattering from the Proton”. In: *Phys. Rev.* 98 (1 1955), pp. 217–218.
- [Xio+19] W. Xiong et al. “A small proton charge radius from an electron–proton scattering experiment”. In: *Nature* 575.7781 (2019), pp. 147–150.

- [Kha21] Dmitri E. Kharzeev. “Mass radius of the proton”. In: *Phys. Rev. D* 104 (5 2021), p. 054015.
- [Adh+23a] S. Adhikari et al. “Measurement of the  $J/\psi$  photoproduction cross section over the full near-threshold kinematic region”. In: *Phys. Rev. C* 108.2 (2023), p. 025201.
- [Dur+23] B. Duran et al. “Determining the gluonic gravitational form factors of the proton”. In: *Nature* 615.7954 (2023), pp. 813–816.
- [MC22] Victor I. Mokeev and Daniel S. Carman. “Photo- and Electrocouplings of Nucleon Resonances”. In: *Few Body Syst.* 63.3 (2022), p. 59.
- [Gro+23] Franz Gross et al. “50 Years of Quantum Chromodynamics”. In: *Eur. Phys. J. C* 83 (2023), p. 1125.
- [Car+23] Daniel S. Carman et al. “Nucleon Resonance Electroexcitation Amplitudes and Emergent Hadron Mass”. In: *Particles* 6.1 (2023), pp. 416–439.
- [DRS23] Minghui Ding, Craig D. Roberts, and Sebastian M. Schmidt. “Emergence of Hadron Mass and Structure”. In: *Particles* 6 (2023), pp. 57–120.
- [HMM23] A. N. Hiller Blin, V. I. Mokeev, and W. Melnitchouk. “Resonant contributions to polarized proton structure functions”. In: *Phys. Rev. C* 107.3 (2023), p. 035202.
- [Hil+19] A. N. Hiller Blin et al. “Nucleon resonance contributions to unpolarised inclusive electron scattering”. In: *Phys. Rev. C* 100.3 (2019), p. 035201.
- [Hil+21] A. N. Hiller Blin et al. “Resonant contributions to inclusive nucleon structure functions from exclusive meson electroproduction data”. In: *Phys. Rev. C* 104.2 (2021), p. 025201.
- [Ado+15] C. Adolph et al. In: *Phys. Lett.* B740 (2015), pp. 303–311.
- [Agh+18] M. Aghasyan et al. In: *Phys.Rev.* D98.9 (2018), p. 092003.
- [Rod+19] A. Rodas et al. In: *Phys. Rev. Lett.* 122.4 (2019), p. 042002.
- [Dud11] J. J. Dudek. In: *Phys. Rev.* D84 (2011), p. 074023.
- [SK06] A. P. Szczepaniak and P. Krupinski. In: *Phys. Rev.* D73 (2006), p. 116002.
- [GYS14] P. Guo, T. Yépez-Martínez, and A. P. Szczepaniak. In: *Phys. Rev.* D89.11 (2014), p. 116005.
- [MFS15] V. Mathieu, G. Fox, and A. P. Szczepaniak. In: *Phys.Rev.* D92.7 (2015), p. 074013.
- [Nys+18] J. Nys et al. In: *Phys.Lett.* B779 (2018), pp. 77–81.
- [Mat+20] V. Mathieu et al. “Exclusive tensor meson photoproduction”. 2020. arXiv: 2005.01617 [hep-ph].
- [PR20] J.R. Peláez and A. Rodas. In: *Phys. Rev. Lett.* 124.17 (2020), p. 172001.
- [Bri+17] R. A. Briceño et al. In: *Phys.Rev.Lett.* 118.2 (2017), p. 022002.
- [Wil+19] David J. Wilson et al. In: *Phys. Rev. Lett.* 123.4 (2019), p. 042002.
- [Gia+05] F. Giacosa et al. In: *Phys. Rev.* D72 (2005), p. 094006.
- [KZ07] E. Klempt and A. Zaitsev. In: *Phys. Rept.* 454 (2007), pp. 1–202.
- [Pil+18] A. Pilloni et al. In: *Eur.Phys.J.* C78.9 (2018), p. 727.
- [Mik+20] M. Mikhasenko et al. In: *Phys. Rev.* D101.3 (2020), p. 034033.
- [Pau+18] P. Pauli et al. In: *Phys. Rev.* C98.6 (2018), p. 065201.
- [Mat+19] V. Mathieu et al. In: *Phys.Rev.* D100.5 (2019), p. 054017.
- [Smi+23] W. A. Smith et al. “Ambiguities in partial wave analysis of two spinless meson photoproduction”. In: *Phys. Rev. D* 108 (7 2023), p. 076001.

- [Adh+23b] S. Adhikari et al. “Measurement of spin-density matrix elements in  $\rho(770)$  production with a linearly polarized photon beam at  $E_\gamma = 8.2 - 8.8\text{GeV}$ ”. In: *Phys. Rev. C* 108 (5 2023), p. 055204.
- [Alg+23] T. Alghamdi et al. “Toward a generative modeling analysis of CLAS exclusive  $2\pi$  photoproduction”. In: *Phys. Rev. D* 108 (9 2023), p. 094030.
- [Abe+85] K. Abe et al. “Inclusive Photoproduction of Strange Baryons at 20-GeV”. In: *Phys. Rev. D* 32 (1985), pp. 2869–2882.
- [Sum+19a] M. Sumihama et al. In: *Phys. Rev. Lett.* 122 (7 2019), p. 072501.
- [Guo+07] L. Guo et al. In: *Phys. Rev. C* 76 (2 2007), p. 025208.
- [Sum+19b] M. Sumihama et al. “Observation of  $\Xi(1620)^0$  and evidence for  $\Xi(1690)^0$  in  $\Xi_c^+ \rightarrow \Xi^- \pi^+ \pi^+$  decays”. In: *Phys. Rev. Lett.* 122.7 (2019), p. 072501.
- [NH24] Takuma Nishibuchi and Tetsuo Hyodo. “Analysis of  $\Xi(1620)$  resonance with chiral unitary approach”. In: *EPJ Web Conf.* 291 (2024), p. 05006.
- [Mok+20] V.I. Mokeev et al. In: *Phys. Lett. B* 805 (2020), p. 135457.
- [Sad+23] Daniel Sadasivan et al. “New insights into the pole parameters of the  $\Lambda(1380)$ , the  $\Lambda(1405)$  and the  $\Sigma(1385)$ ”. In: *Front. Phys.* 11 (2023), p. 1139236.
- [Goe18] J. T. et al. Goetz. In: *Phys. Rev. C* 98 (6 2018), p. 062201.
- [Ama+20] Moskov Amaryan et al. “Strange Hadron Spectroscopy with Secondary KL Beam in Hall D”. In: (2020). arXiv: 2008.08215 [nucl-ex].